Neutrons and X-rays in magnetism

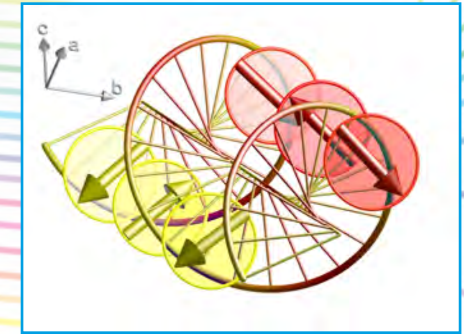

Navid Qureshi

Motivation

Problem ⟶ Method

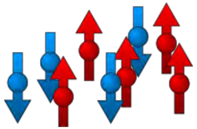

simple magnetic structures
and *large* magnetic moments

powder diffraction

complex magnetic structures
and/or *small* magnetic moments

single-crystal diffraction

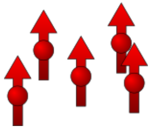

spin density maps
and non-spherical models

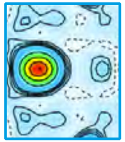

flipping ratio method

separate nuclear/magnetic scattering
and directional information

	NSF	SF
$\mathbf{P}_0 \parallel x$	σ_N	$\sigma_{M_y} + \sigma_{M_z}$
$\mathbf{P}_0 \parallel y$	$\sigma_N + \sigma_{M_y}$	σ_{M_z}
$\mathbf{P}_0 \parallel z$	$\sigma_N + \sigma_{M_z}$	σ_{M_y}

longitudinal polarization analysis

complex magnetic structures,
cs separation and chiralities

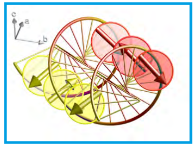

spherical neutron polarimetry

Motivation

Problem → Method

Complexity scale

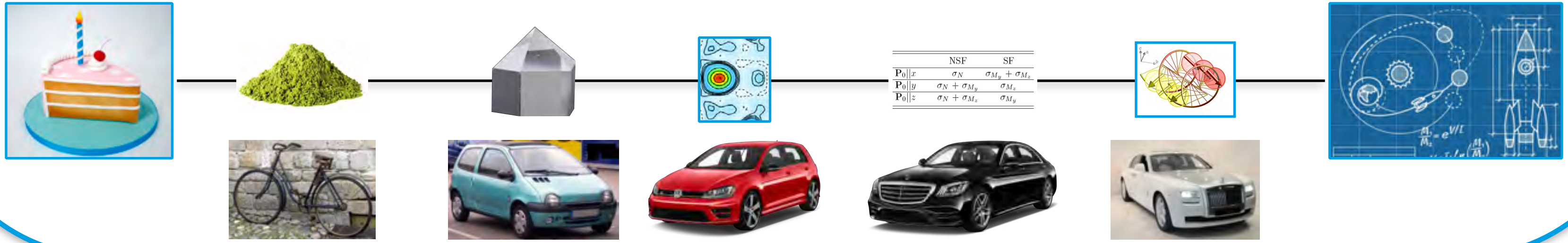

	NSF	SF
$\mathbf{P}_0 \| x$	σ_N	$\sigma_{M_y} + \sigma_{M_z}$
$\mathbf{P}_0 \| y$	$\sigma_N + \sigma_{M_y}$	σ_{M_z}
$\mathbf{P}_0 \| z$	$\sigma_N + \sigma_{M_z}$	σ_{M_y}

Magnetic structures

Powder diffraction

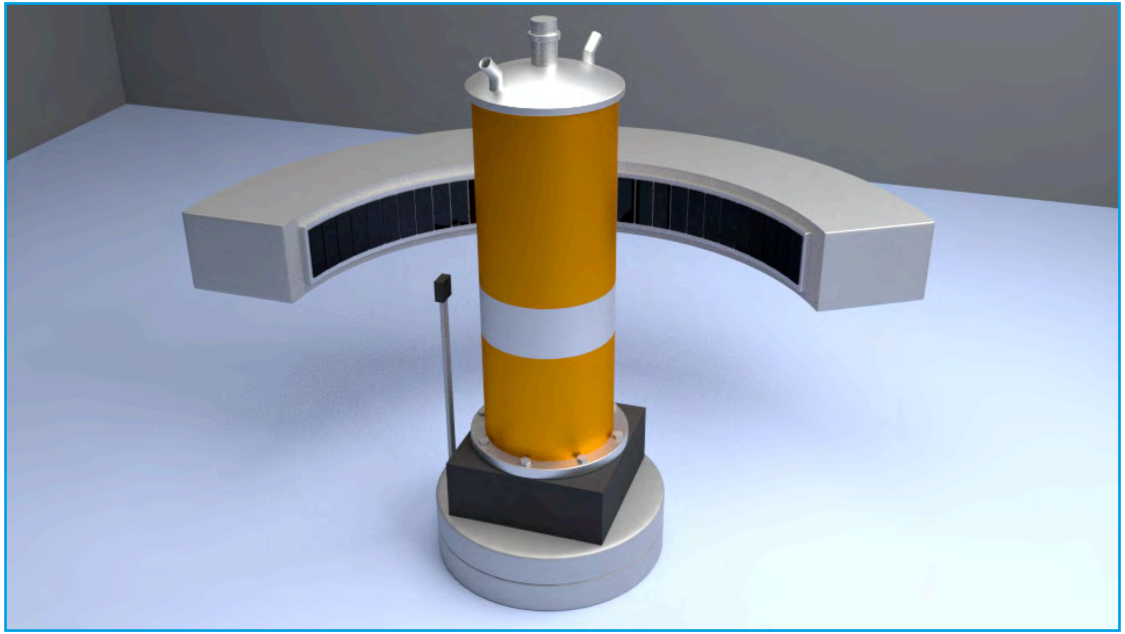

Magnetic structures

Powder diffraction

Result: Diffraction pattern

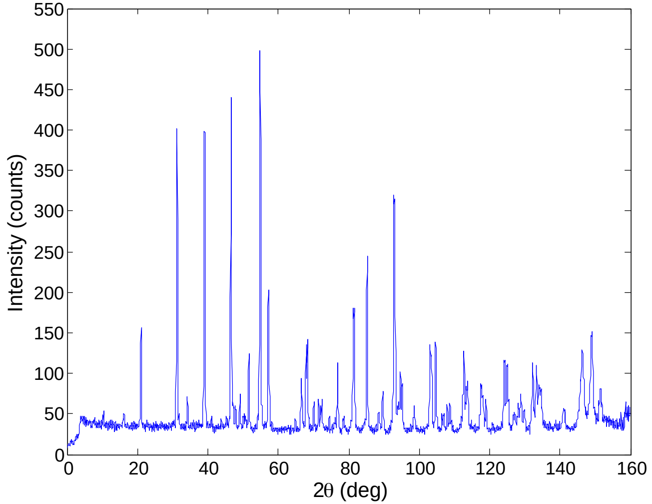

Useful information lies in the

- position
- the intensity
- the shape and width

of the reflections.

Downsides:

- not always easy to find **q**
- superposition of peaks
- magnetic *equivalents* not equivalent

Magnetic structures

Powder diffraction

Result: Diffraction pattern

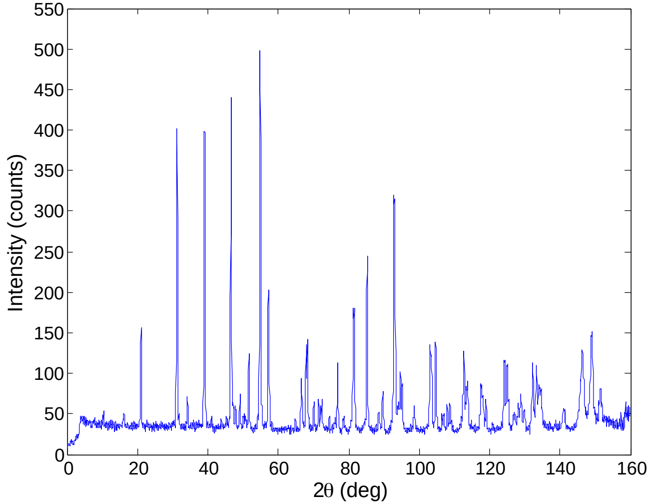

Useful information lies in the

- position
- the intensity
- the shape and width

of the reflections.

Downsides:

- not always easy to find **q**
- superposition of peaks
- magnetic *equivalents* not equivalent

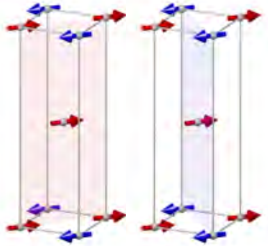

Magnetic structures

Powder diffraction - ambiguity

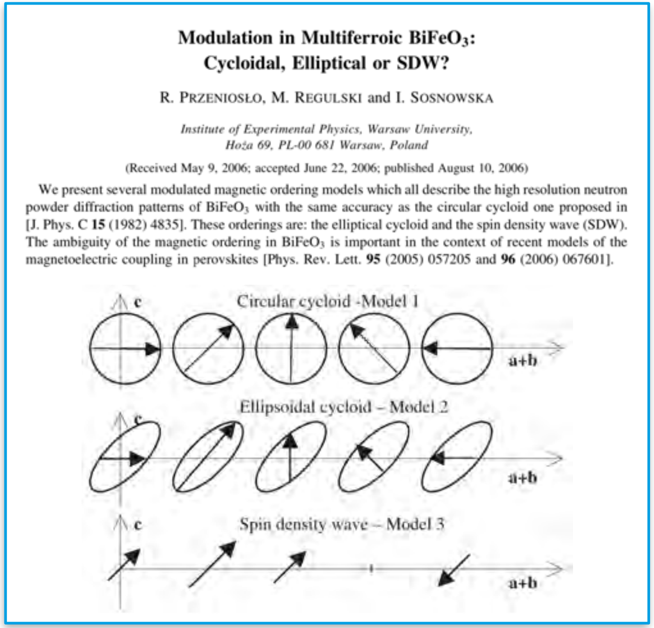

Modulation in Multiferroic $BiFeO_3$: Cycloidal, Elliptical or SDW?

R. Przeniosło, M. Regulski and I. Sosnowska

Institute of Experimental Physics, Warsaw University, Hoża 69, PL-00 681 Warsaw, Poland

(Received May 9, 2006; accepted June 22, 2006; published August 10, 2006)

We present several modulated magnetic ordering models which all describe the high resolution neutron powder diffraction patterns of $BiFeO_3$ with the same accuracy as the circular cycloid one proposed in [J. Phys. C **15** (1982) 4835]. These orderings are: the elliptical cycloid and the spin density wave (SDW). The ambiguity of the magnetic ordering in $BiFeO_3$ is important in the context of recent models of the magnetoelectric coupling in perovskites [Phys. Rev. Lett. **95** (2005) 057205 and **96** (2006) 067601].

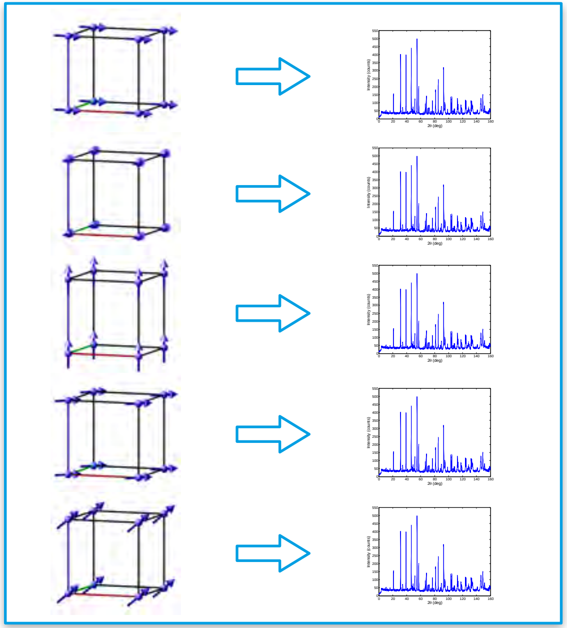

Magnetic structures

Magnetic ordering in manganates

Radaelli et al., Phys. Rev. B **55** 3015 (1997)

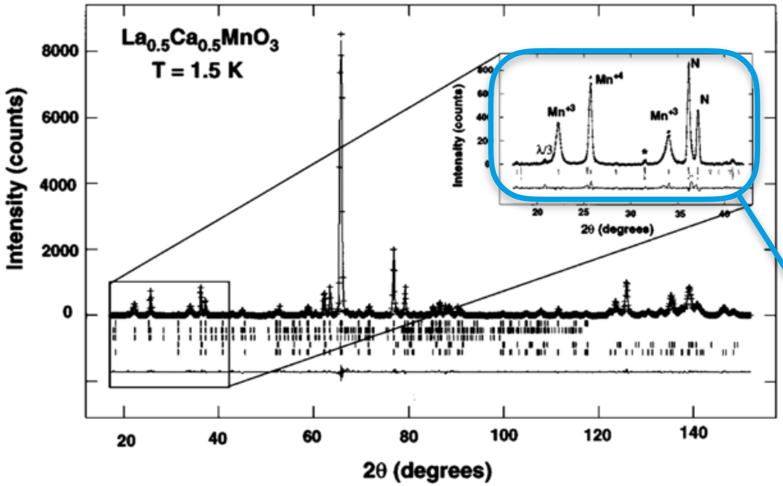

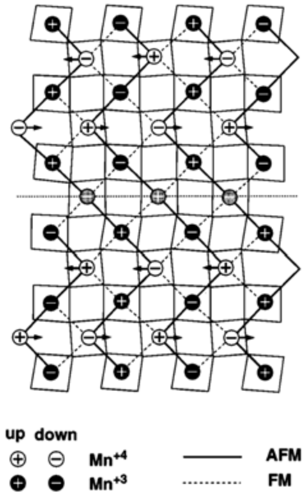

2. Different moment directions for Mn^{3+} and Mn^{4+}

3. Spin-flip domain boundaries in Mn^{3+} structure

1. Different modulations for Mn^{3+} and Mn^{4+} sub lattices

Magnetic structures

Single crystal diffraction - 4-circle geometry

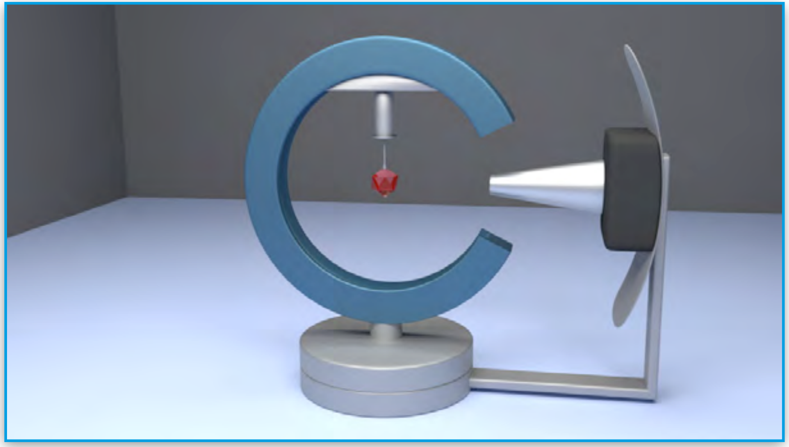

by adjusting 2θ, ω, χ and ϕ

the sample is put in reflection position

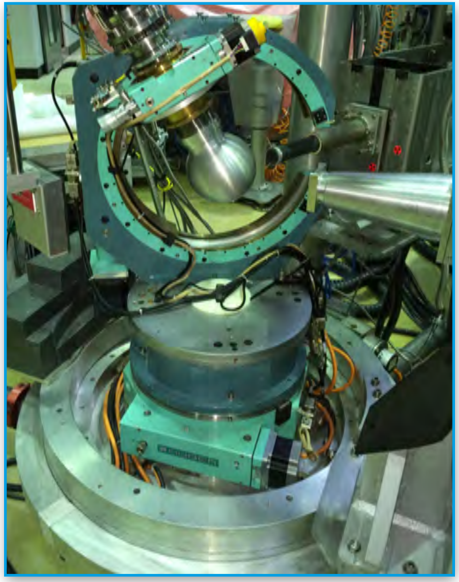

D10 (ILL)

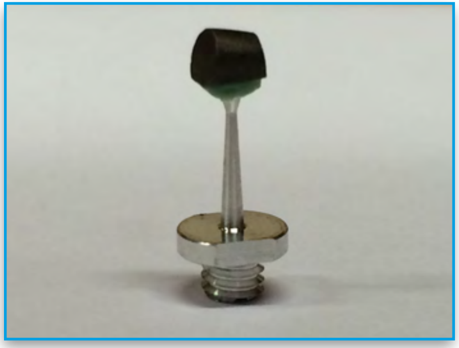

single crystal on Al pin

Magnetic structures

Single crystal diffraction - Normal beam geometry

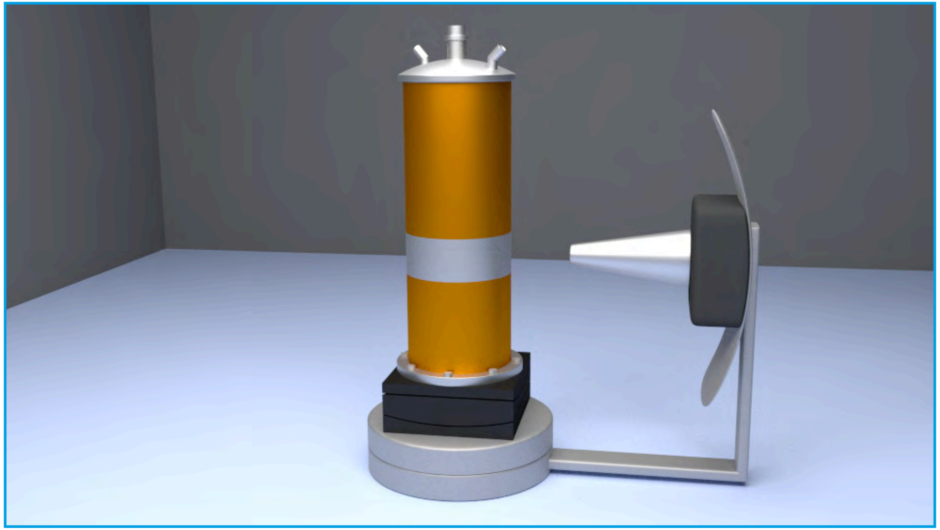

cryomagnets, pressure cells, …
cannot be tilted much

→ confined to the scattering plane
e.g. only (*hk*0) reflections

→ lifting counter
able to reach l=1, 2…

Magnetic structures

Magnetic ordering in $Ni_3V_2O_8$

Lawes et al., Phys. Rev. Lett. **93** 247201 (2004)

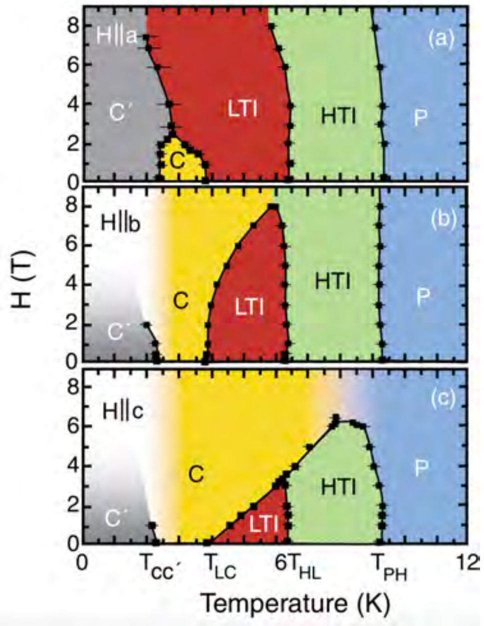

Lawes et al., Phys. Rev. Lett. **95** 087205 (2005)

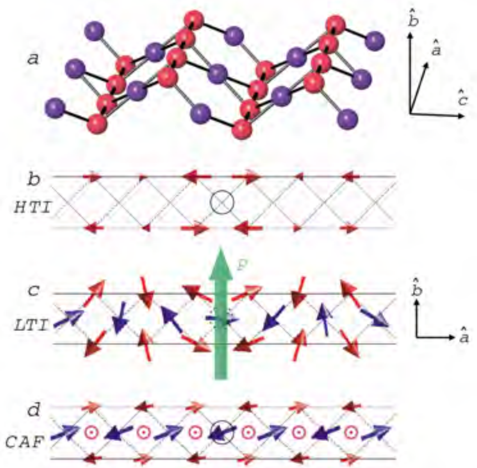

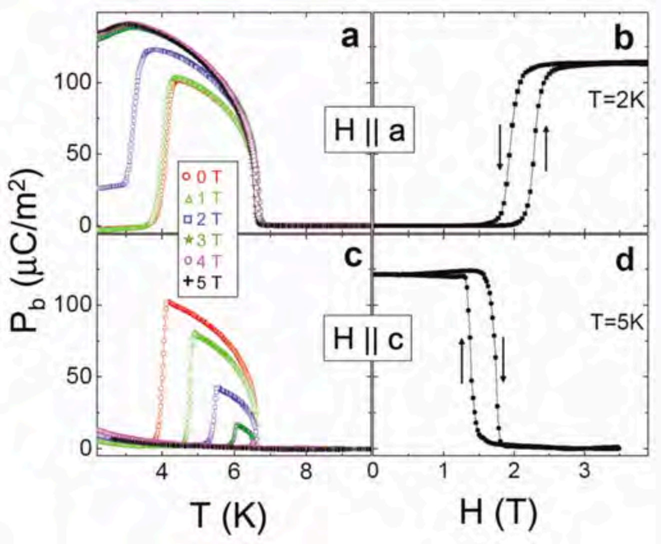

complex **cycloidal** magnetic structure breaks inversion symmetry and induces macroscopic electric polarisation → **multiferroic**

Magnetic structures

Comparison: Powder vs. single crystal diffraction

- straightforward experiment
- Rietveld analysis (profile)
- no knowledge on structure required
- peak overlap
- loss of vectorial information

- requires knowledge on structure
- list of (hkl) and intensities
- peaks measured individually
- no loss of vectorial information
- Extinction
- magnetic domains

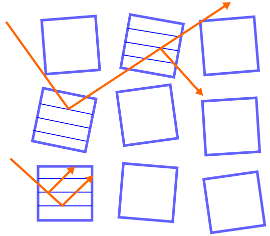

Magnetic structures

Comparison: Powder vs. single crystal diffraction

- straightforward experiment
- Rietveld analysis (profile)
- no knowledge on structure required
- peak overlap
- loss of vectorial information

- requires knowledge on structure
- list of (hkl) and intensities
- peaks measured individually
- no loss of vectorial information
- Extinction
- magnetic domains

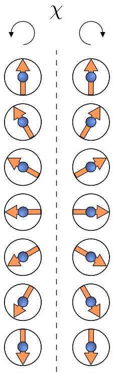

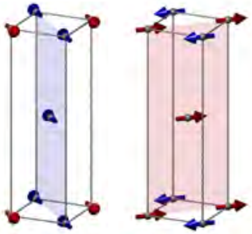

Magnetic structures

Non-resonant magnetic X-ray diffraction

- At 1 keV magnetic scattering cross section is $3.8*10^{-6}$ smaller than Thomson scattering
- Only a few unpaired electrons contribute to magnetic scattering, while all electrons to Thomson scattering
- however, large flux largely compensates for small cross sections
- Magnetic scattering (and L/S) has different polarization dependence than Thomson scattering
- spin and orbital moment can be distinguished
- microfocussing down to 20 nm

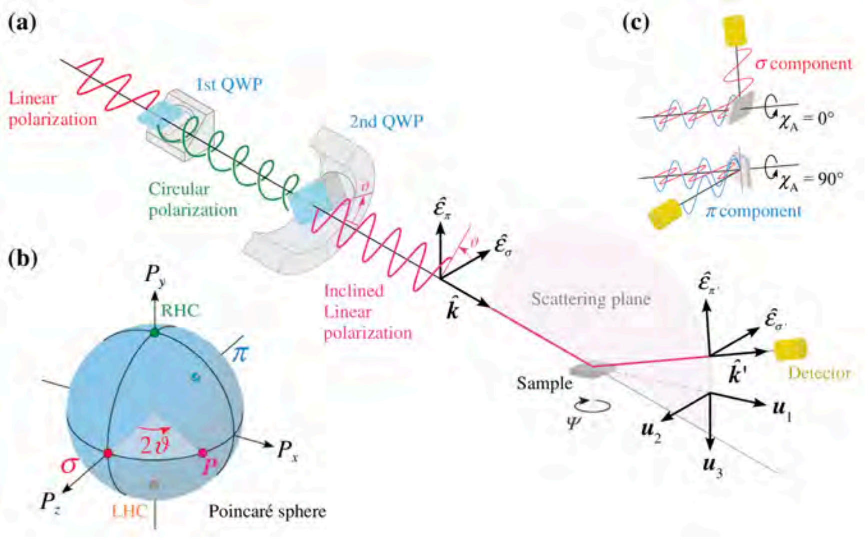

Ohsumi and Arima, Advances in Physics: X **1** 128 (2016)

Magnetic structures

Non-resonant magnetic X-ray diffraction

- use of X-ray polarisation to deduce spin-rotation plane
- magnetic structure refinement to unpolarised neutron data

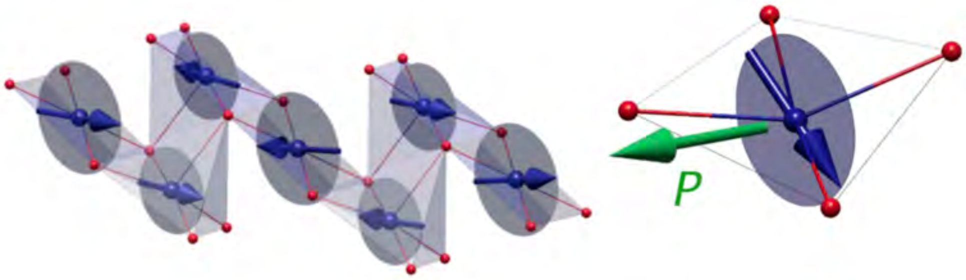

Johnson et al., Phys. Rev. Lett. **107** 137205 (2011)

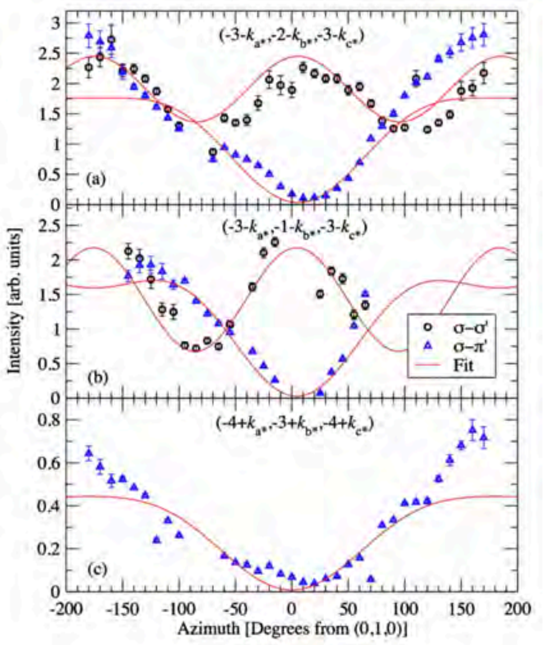

Magnetic structures

Non-resonant magnetic X-ray diffraction

- microfocusing allows to probe individual magnetic domains

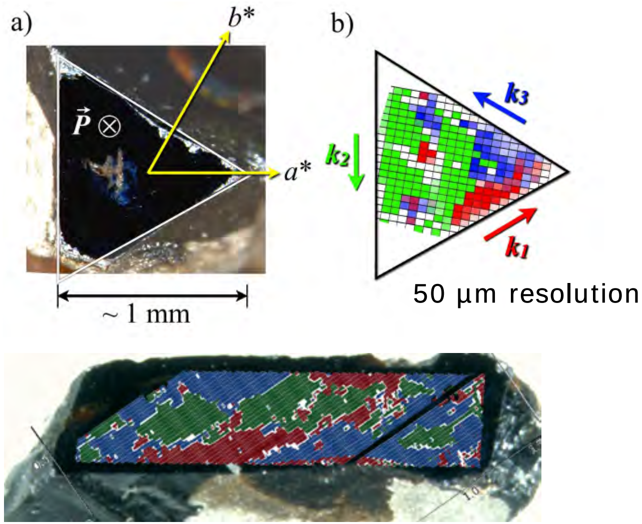

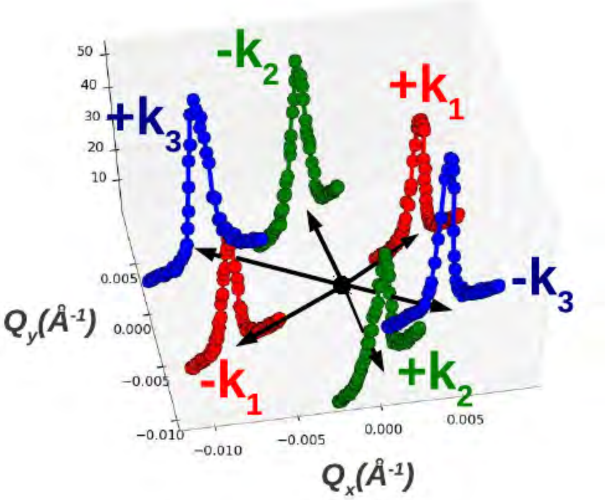

Johnson et al., Phys. Rev. Lett. **110** 217206 (2011)

Magnetic structures

Resonant magnetic X-ray diffraction

- Tune the energy of the X-ray beam to an absorption edge
- Photon is absorbed and the system re-emits a photon with the same energy
- Element-specific information
- Combination of spectroscopy technique with Bragg scattering
- Ideal example: $GdMn_2O_5$
- Gd and Mn order
- Gd has huge neutron absorption cross section

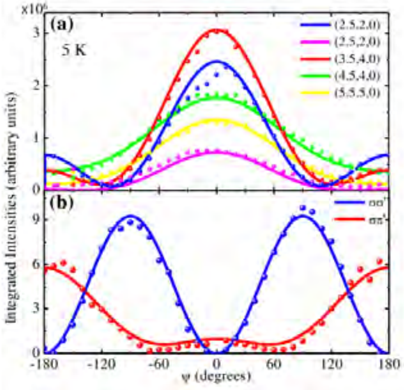

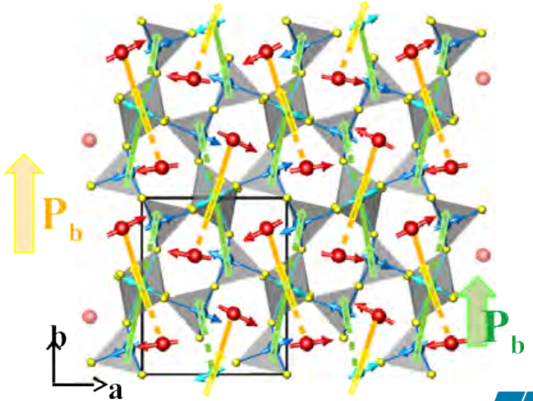

Lee et al., Phys. Rev. Lett. **110** 137203 (2013)

Polarized neutrons

Why use them?

neutron spin state can be different after scattering process depending on interaction

Rules:

1. Nuclear scattering is always a non-spin-flip process
2. Only the component $\mathbf{F}_M \perp \mathbf{Q}$ contributes to magnetic scattering
3. The magnetic component $\mathbf{F}_M \perp \mathbf{P}_i$ contributes to spin-flip scattering
4. The magnetic component $\mathbf{F}_M \parallel \mathbf{P}_i$ contributes to non-spin-flip scattering

	NSF	SF
$\mathbf{P}_0 \Vert x$	σ_N	$\sigma_{M_y} + \sigma_{M_z}$
$\mathbf{P}_0 \Vert y$	$\sigma_N + \sigma_{M_y}$	σ_{M_z}
$\mathbf{P}_0 \Vert z$	$\sigma_N + \sigma_{M_z}$	σ_{M_y}

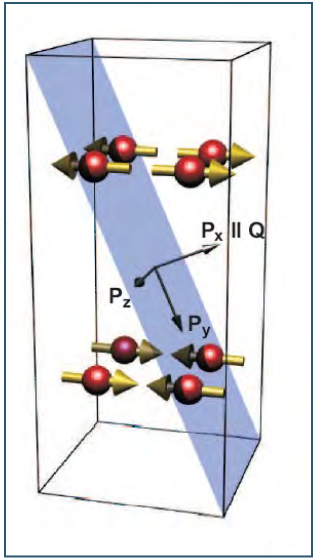

reference frame
[100]-[001] scattering plane

Spin densities

Flipping ratio method

- sensitive technique used to derive spin density maps
- accurate $\mathbf{F}_M$ allow a non-spherical model of the spin distribution
- accuracy due to interference term

E.g.: $F_M = 0.1 \cdot F_N$

unpolarized: $F_N^2 + F_M^2 = 1.01 F_N^2$

polarized: $(F_N + F_M)^2 = F_N^2 + 2F_N F_M + F_M^2 = 1.21 F_N^2$

flipping ratio: $R = \dfrac{I^+}{I^-} = \dfrac{1.21}{0.81} \approx 1.25$

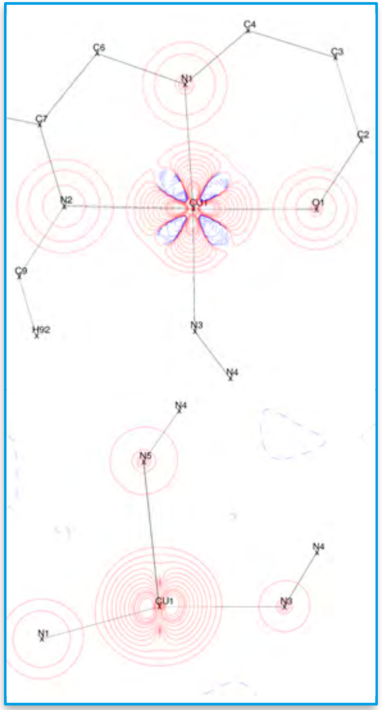

Lecomte et al., ACA Transactions (2011)

spin density in double-bridged Cu complex

significant population of d_{z^2} and $d_{x^2-y^2}$

Spin densities

Flipping ratio method

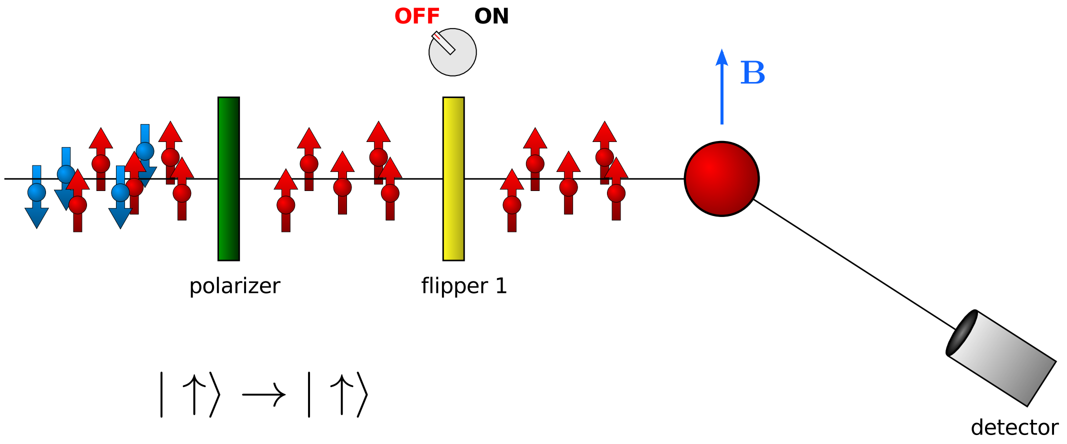

	NSF	SF
$\mathbf{P}_0 \parallel x$	σ_N	$\sigma_{M_y} + \sigma_{M_z}$
$\mathbf{P}_0 \parallel y$	$\sigma_N + \sigma_{M_y}$	σ_{M_z}
$\mathbf{P}_0 \parallel z$	$\sigma_N + \sigma_{M_z}$	σ_{M_y}

$$|\uparrow\rangle \rightarrow |\uparrow\rangle$$

x and y within scattering plane
z vertical

Spin densities

Flipping ratio method

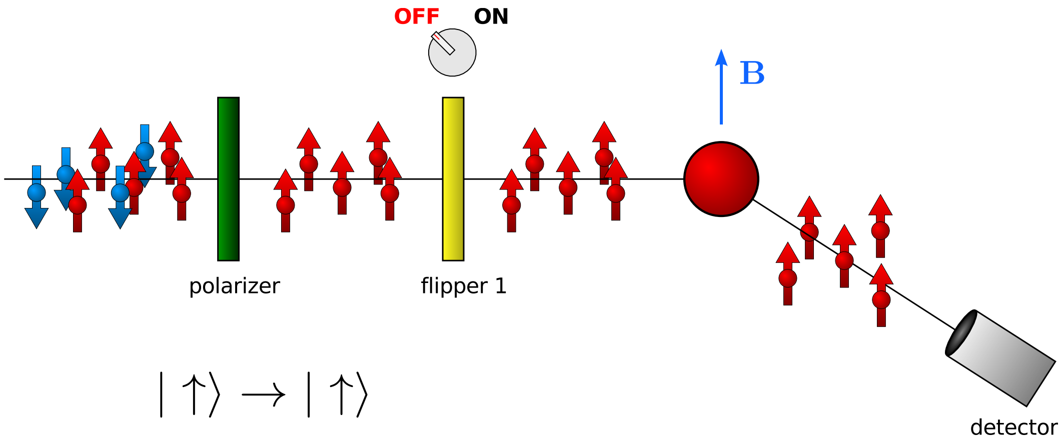

$$|\uparrow\rangle \rightarrow |\uparrow\rangle$$

$$(F_N + F_M)^2$$

	NSF	SF
$\mathbf{P}_0 \| x$	σ_N	$\sigma_{M_y} + \sigma_{M_z}$
$\mathbf{P}_0 \| y$	$\sigma_N + \sigma_{M_y}$	σ_{M_z}
$\mathbf{P}_0 \| z$	$\sigma_N + \sigma_{M_z}$	σ_{M_y}

x and y within scattering plane
z vertical

only non-spin-flip scattering

Spin densities

Flipping ratio method

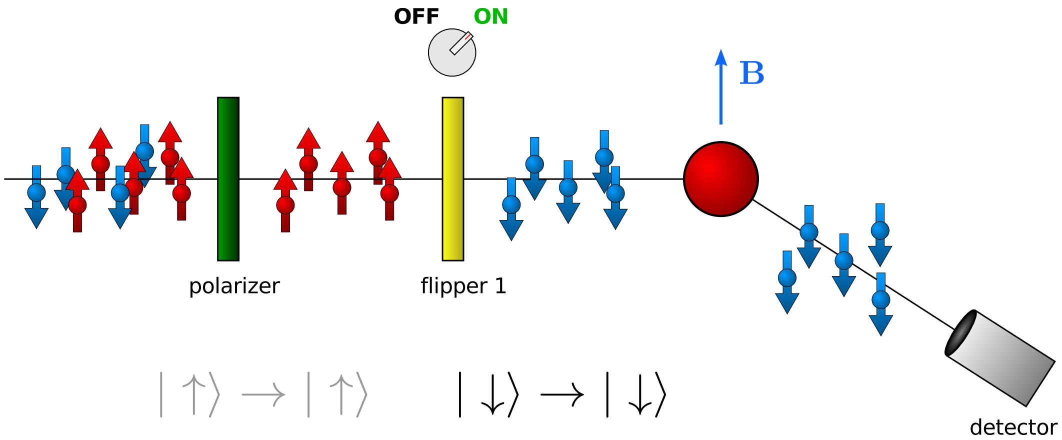

$|\uparrow\rangle \rightarrow |\uparrow\rangle$ $\quad |\downarrow\rangle \rightarrow |\downarrow\rangle$

$(F_N - F_M)^2$

	NSF	SF
$\mathbf{P}_0 \| x$	σ_N	$\sigma_{M_y} + \sigma_{M_z}$
$\mathbf{P}_0 \| y$	$\sigma_N + \sigma_{M_y}$	σ_{M_z}
$\mathbf{P}_0 \| z$	$\sigma_N + \sigma_{M_z}$	σ_{M_y}

x and y within scattering plane
z vertical

only non-spin-flip scattering

Spin densities

Magnetic Compton scattering

- Incoherent scattering technique using circularly polarised X-rays
- based on well-known Compton effect
- one can measure the projection of all electron momenta on the scattering vector (defined as Compton profile)

$$J(p_z) = \int\int \rho(p_x, p_y, p_z) dp_x dp_y$$

- Total cross section: $\dfrac{\partial^2\sigma}{\partial\Omega\partial\omega_2} \propto |A|^2 J(p_z) + 2i \cdot A^* B \cdot J_{mag}(p_z)$

- Magnetic Compton Profile:

$$J_{mag}(p_z) = \int\int |\chi_\uparrow(\mathbf{p})|^2 - |\chi_\downarrow(\mathbf{p})|^2 = \int\int \rho_{mag}(\mathbf{p}) dp_x dp_y$$

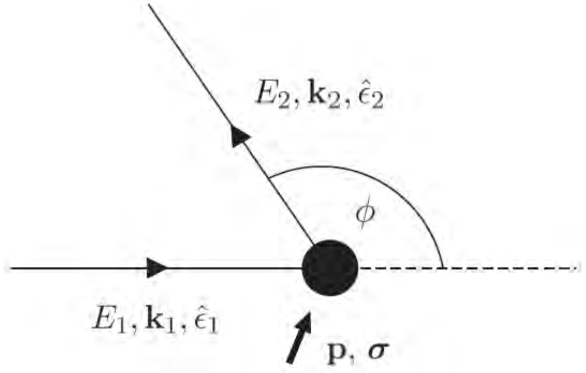

$$E_2 - E_1 = \hbar\omega = \frac{1}{2m}[\mathbf{p} + \hbar(\mathbf{k}_1 - \mathbf{k}_2)]^2 - \frac{|\mathbf{p}|^2}{2m}$$

$$= \boxed{\frac{\hbar^2\mathbf{q}^2}{2m}} + \boxed{\frac{\hbar\mathbf{q}\cdot\mathbf{p}}{m}}$$

Compton shift projection of **p** on **q**

Spin densities

Magnetic Compton scattering

- Incoherent scattering technique using circularly polarised X-rays
- based on well-known Compton effect
- one can measure the projection of all electron momenta on the scattering vector (defined as Compton profile)

$$J(p_z) = \int\int \rho(p_x, p_y, p_z) dp_x dp_y$$

- Total cross section: $\frac{\partial^2 \sigma}{\partial\Omega\partial\omega_2} \propto |A|^2 J(p_z) + 2i \cdot A^* B \cdot J_{mag}(p_z)$

- Magnetic Compton Profile:

$$J_{mag}(p_z) = \int\int |\chi_\uparrow(\mathbf{p})|^2 - |\chi_\downarrow(\mathbf{p})|^2 = \int\int \rho_{mag}(\mathbf{p}) dp_x dp_y$$

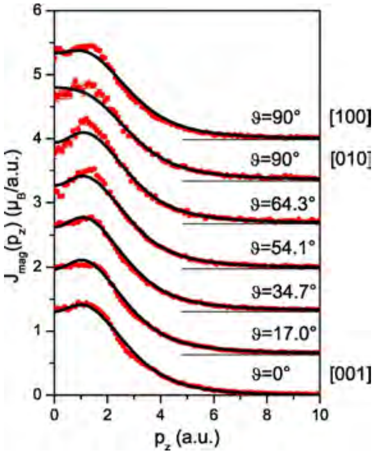

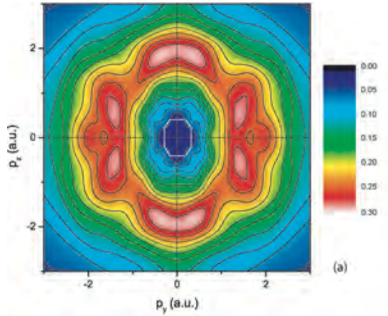

momentum density in $Co_3V_2O_8$

Spin densities

Correlation of real and momentum space

Spin polarized orbital occupation

Real space

$$f_a(\mathbf{k}) = \int_{-\infty}^{\infty} \rho_{mag,a}(\mathbf{r}) \exp(2\pi i \mathbf{k}\mathbf{r}) d\mathbf{r}$$

$$\rho_{mag,a}(\mathbf{r}) = \sum_m \beta_m \psi^2_{m,a}(\mathbf{r})$$

Momentum space

$$J_{mag}(p_z) = \int_{-\infty}^{\infty}\int_{-\infty}^{\infty} \rho_{mag}(\mathbf{p}) dp_x dp_y$$

$$\rho_{mag}(\mathbf{p}) = \sum_m \beta_m \chi^2_m(\mathbf{p})$$

Ab initio MO wave functions

$$\psi(\mathbf{r}) = FT[\chi(\mathbf{p})]$$

Spin densities

Correlation of real and momentum space

Spin polarized orbital occupation

Real space

Momentum space

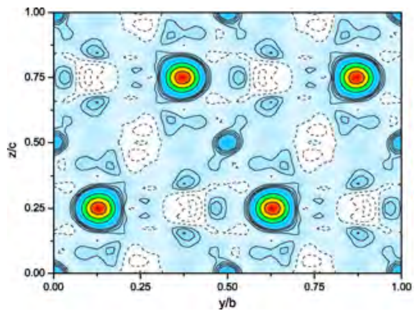

observed

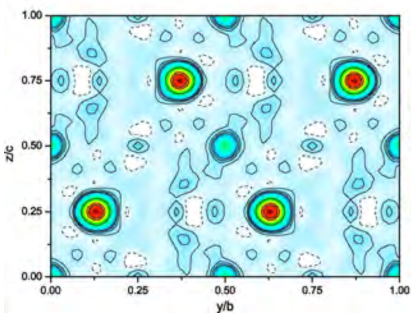

calculated

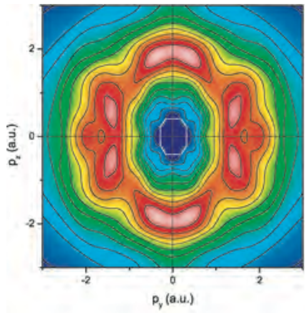

observed

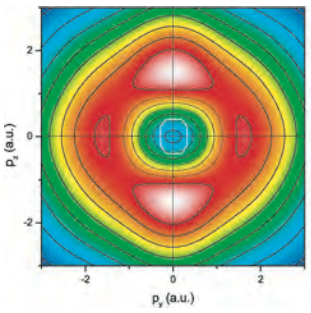

calculated

→ orbital occupations, super-exchange pathways, hybridization, etc.

Polarized analysis

Neutrons

More information can be extracted by analysing the final polarization of the neutrons.

	NSF	SF
$\mathbf{P}_0 \| x$	σ_N	$\sigma_{M_y} + \sigma_{M_z}$
$\mathbf{P}_0 \| y$	$\sigma_N + \sigma_{M_y}$	σ_{M_z}
$\mathbf{P}_0 \| z$	$\sigma_N + \sigma_{M_z}$	σ_{M_y}

Longitudinal Polarization Analysis (LPA): set $\mathbf{P}_i$ along x, y or z and analyse the component of $\mathbf{P}_f$ along the same direction

6 possibilities: 3 directions x 2 cross sections

x,y,z $I^{++}(I^{--}), I^{+-}(I^{-+})$

Spherical Neutron Polarimetry (SNP): set $\mathbf{P}_i$ along x, y or z and analyse the component of $\mathbf{P}_f$ along x, y or z

36 possibilities: 3 directions x 3 directions x 4 cross sections

x,y,z x,y,z $I^{++}, I^{--}, I^{+-}, I^{-+}$

Polarized neutrons

LPA experiment

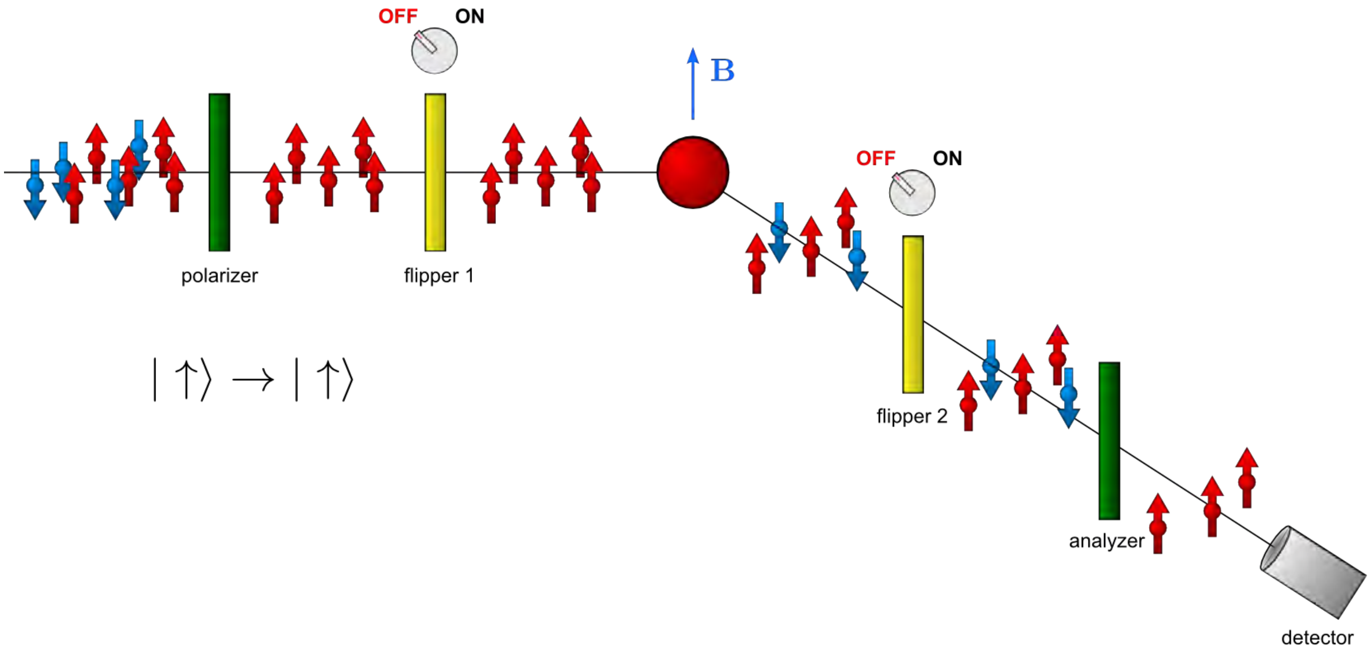

$$|\uparrow\rangle \rightarrow |\uparrow\rangle$$

Polarized neutrons

LPA experiment

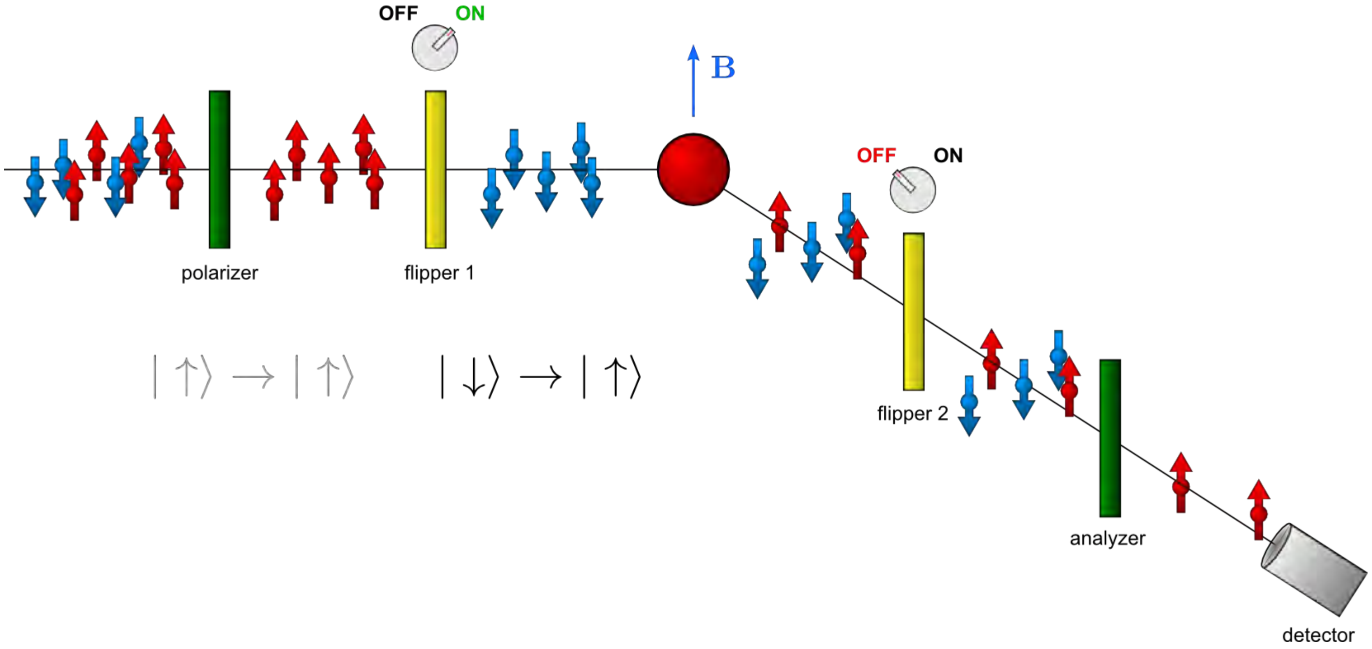

$|\uparrow\rangle \to |\uparrow\rangle$ $|\downarrow\rangle \to |\uparrow\rangle$

Polarized neutrons

LPA experiment

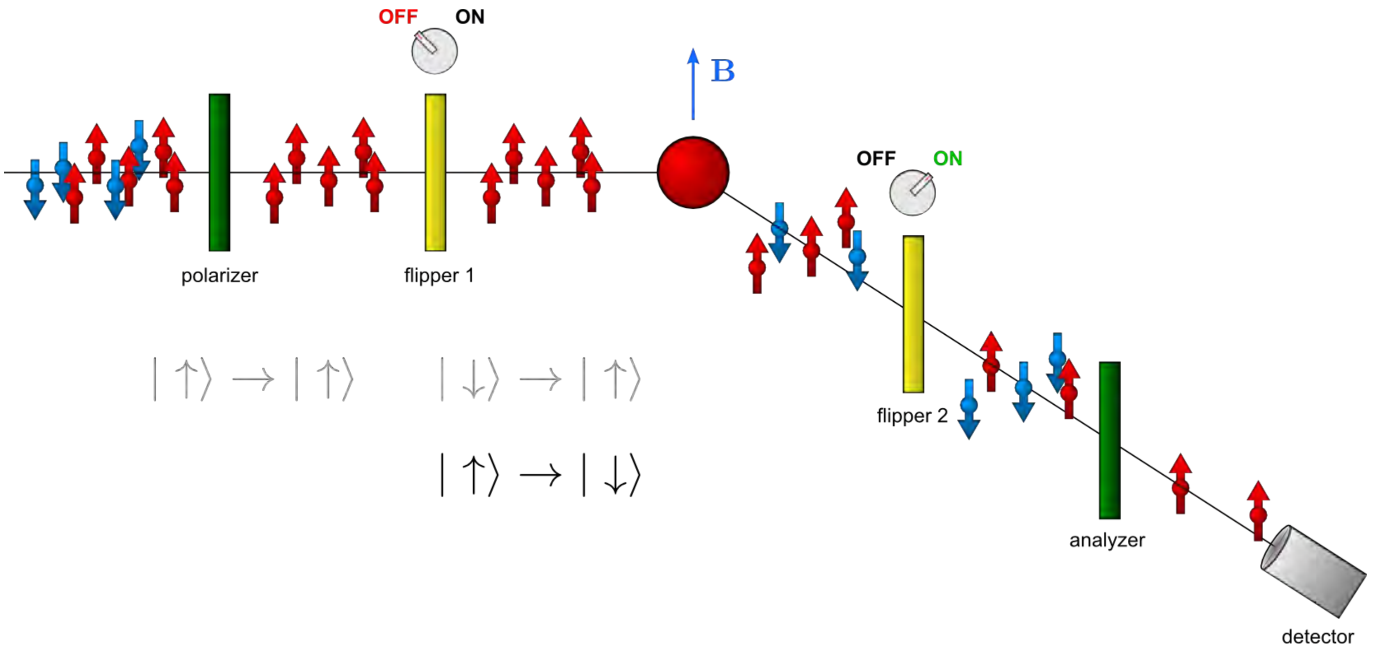

$|\uparrow\rangle \rightarrow |\uparrow\rangle$ $|\downarrow\rangle \rightarrow |\uparrow\rangle$

$|\uparrow\rangle \rightarrow |\downarrow\rangle$

Polarized neutrons

LPA experiment

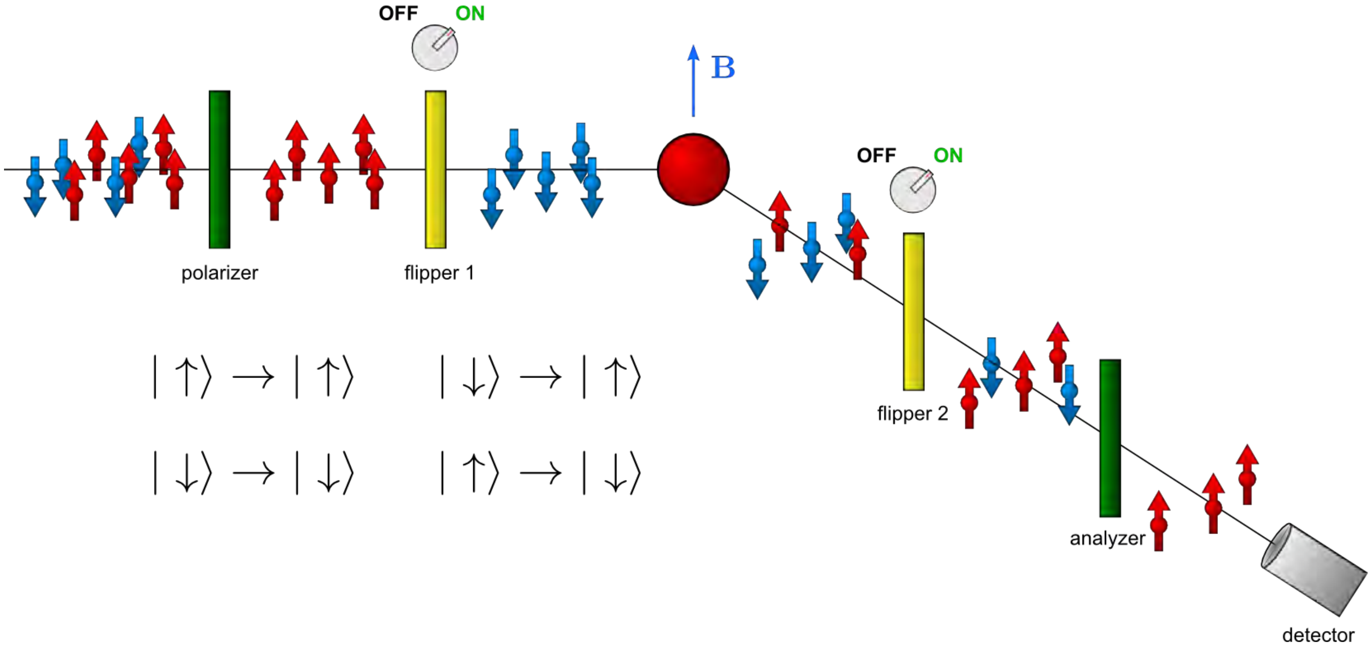

$$|\uparrow\rangle \rightarrow |\uparrow\rangle \qquad |\downarrow\rangle \rightarrow |\uparrow\rangle$$

$$|\downarrow\rangle \rightarrow |\downarrow\rangle \qquad |\uparrow\rangle \rightarrow |\downarrow\rangle$$

Polarized neutrons

Helmholtz coils

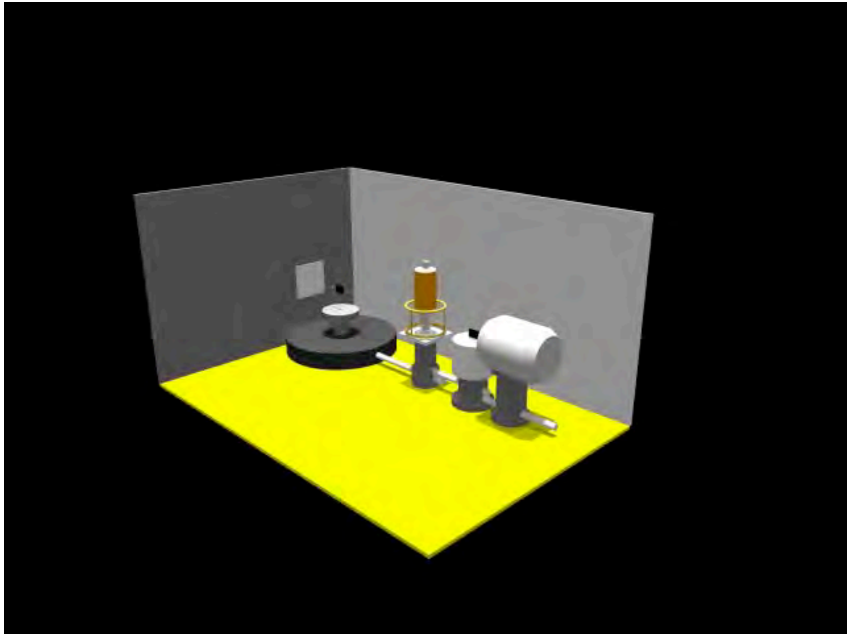

$$\mathbf{P}_i \parallel x$$

$$\mathbf{P}_f \parallel x$$

Polarized neutrons

Spherical neutron polarimetry

Powerful technique used to determine …

- complex magnetic structures
- chiral domain populations

by selectively measuring generalized cross sections of a polarised neutron beam with a single-crystal sample.

Possible to reconstruct the 3D rotation [and (de)polarisation] of the neutron spin.

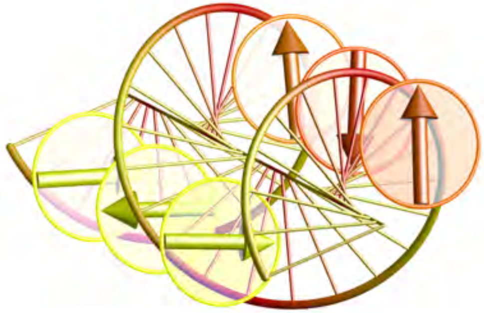

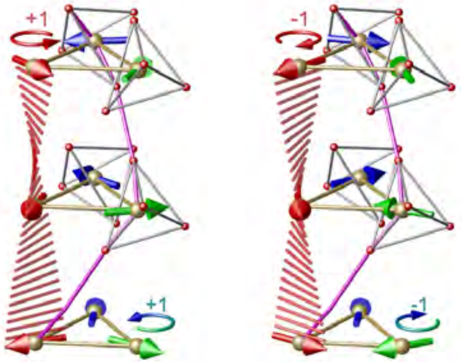

Polarized neutrons

Spherical neutron polarimetry

Powerful technique used to determine …

- complex magnetic structures
- chiral domain populations

by selectively measuring generalized cross sections of a polarised neutron beam with a single-crystal sample.

Possible to reconstruct the 3D rotation [and (de)polarisation] of the neutron spin.

Circularly polarised X-rays

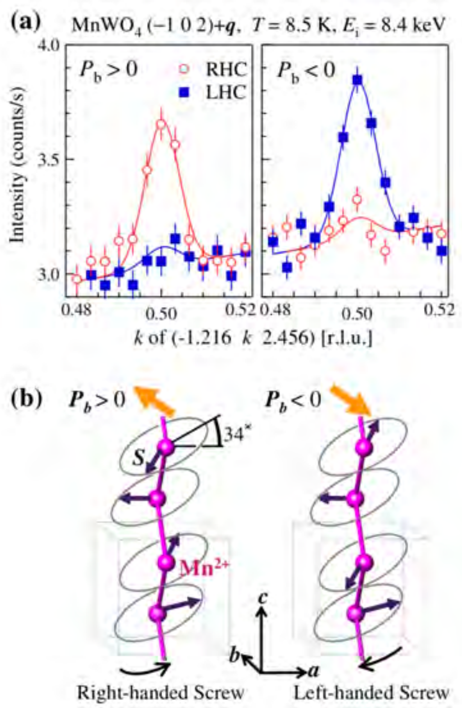

Sagayama et al., J. Phys. Soc. Jpn. **79** 043711 (2010)

Polarized neutrons

Spherical neutron polarimetry

CRYOgenic **P**olarization **A**nalysis **D**evice

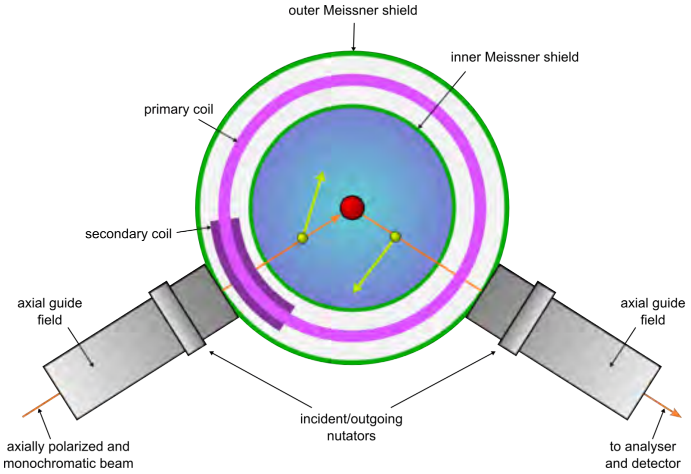

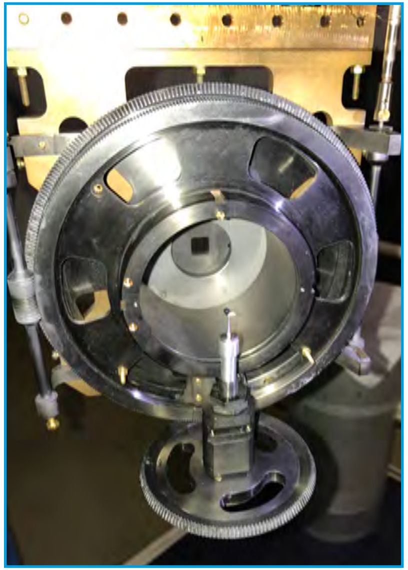

Cryocradle setup allowing for out-of-plane access

Polarized neutrons

Spherical neutron polarimetry

Final neutron polarization is related to initial one by $\mathbf{P}_f = \mathcal{P}\mathbf{P}_i + \mathbf{P}'$

rotational part

created/annihilated polarisation

Polarisation tensor

$$\mathbf{P}_{f,i} = \begin{pmatrix} \frac{\sigma_N - \sigma_{M_{yy}} - \sigma_{M_{zz}} - \sigma_{\chi_x}}{\sigma_x} & \frac{\sigma_{I_{I_z}} - \sigma_{\chi_x}}{\sigma_x} & \frac{\sigma_{I_{I_y}} - \sigma_{\chi_x}}{\sigma_x} \\ \frac{-\sigma_{I_{I_z}} + \sigma_{I_{R_y}}}{\sigma_y} & \frac{\sigma_N + \sigma_{M_{yy}} - \sigma_{M_{zz}} + \sigma_{I_{R_y}}}{\sigma_y} & \frac{\sigma_{M_{yz}} + \sigma_{I_{R_y}}}{\sigma_y} \\ \frac{-\sigma_{I_{I_y}} + \sigma_{I_{R_z}}}{\sigma_z} & \frac{\sigma_{M_{zy}} + \sigma_{I_{R_z}}}{\sigma_z} & \frac{\sigma_N - \sigma_{M_{yy}} + \sigma_{M_{zz}} + \sigma_{I_{R_z}}}{\sigma_z} \end{pmatrix}$$

Local coordination system:

x || **Q**

z vertical

y completes right-handed set

Easily distinguish nuclear, magnetic, chiral and interference terms.

Polarized neutrons

Spherical neutron polarimetry

CRYOgenic **P**olarization **A**nalysis **D**evice

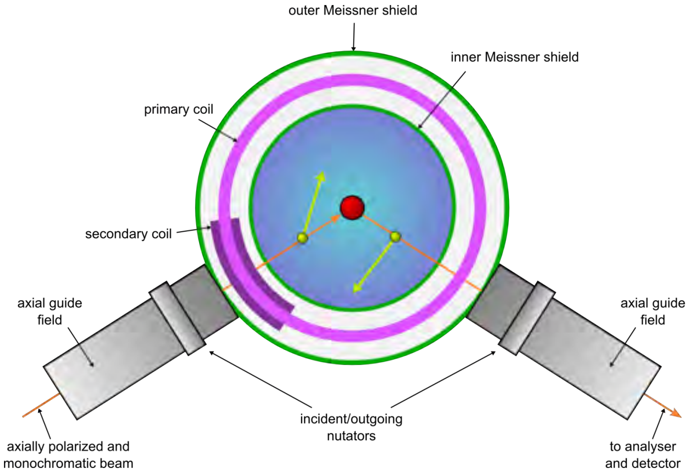

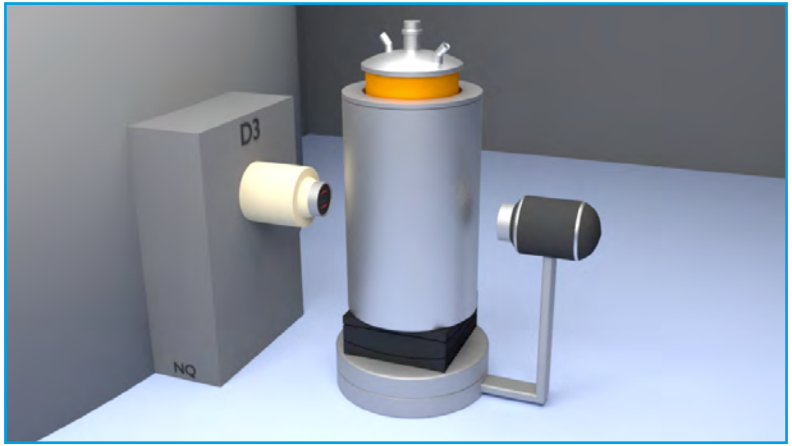

$$\mathbf{P}_i \parallel x \qquad \mathbf{P}_f \parallel y$$

$$P_{f,i} = P_{yx} = \frac{n^+ - n^-}{n^+ + n^-}$$

Magnetic structures

Comparison: Neutron vs. X-ray single crystal diffraction

- Born approximation valid
- Magnetic scattering amplitude comparable to nuclear one
- Large penetration depth -> bulky sample environments
- Manipulation of polarisation and analysis (but costly)
- Large divergence, relatively poor Q-resolution
- Lack of spatial resolution
- No direct L/S separation (only by fitting magnetic form factor)

- No powder
- Off resonance gives quantitative results, but scaling to charge scattering not always easy
- Small magnetic cross section compensated by flux
- Beam heating can be a problem (no dilution)
- Not easy to do k=0 work
- Manipulate polarization and analysis
- Highly collimated, excellent Q-resolution
- Spatial resolution down to 20 nm
- Direct L/S separation
- Element specific information from resonance

Short-range order

Diffuse scattering

- Some magnetic systems do not order even down to very low temperatures
- often bear very interesting physics
- short-range order revealed in diffuse scattering

Short-range order

Diffuse scattering

- Some magnetic systems do not order even down to very low temperatures
- often bear very interesting physics
- short-range order revealed in diffuse scattering
- most prominent example: spin ice
- highly frustrated although ferromagnetic

Bramwell and Gingras, Science **294** 1495 (2001)

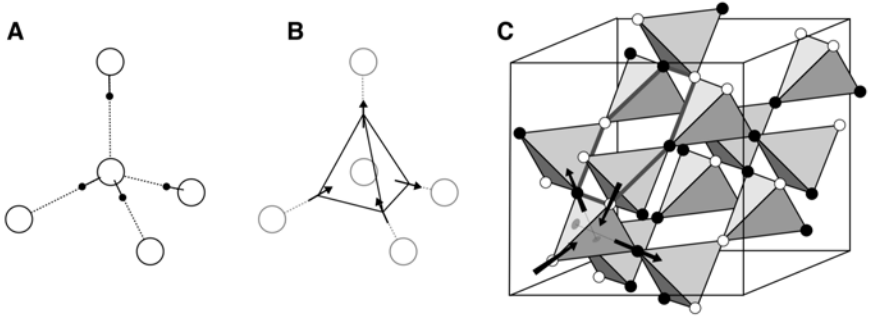

water ice   spin ice   local anisotropy <111>

Short-range order

Diffuse scattering

- Some magnetic systems do not order even down to very low temperatures
- often bear very interesting physics
- short-range order revealed in diffuse scattering
- most prominent example: spin ice
- highly frustrated although ferromagnetic
- *pinch points* in diffuse scattering pattern perfectly reproduced by Monte Carlo analysis

Fennell et al., Science **326** 415 (2009)

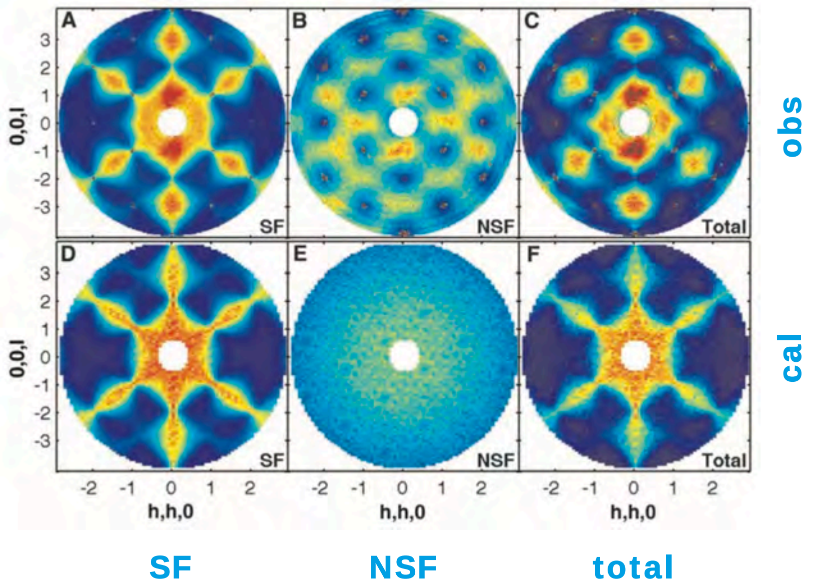

Short-range order

Diffuse scattering

Fennell et al., Science **326** 415 (2009)

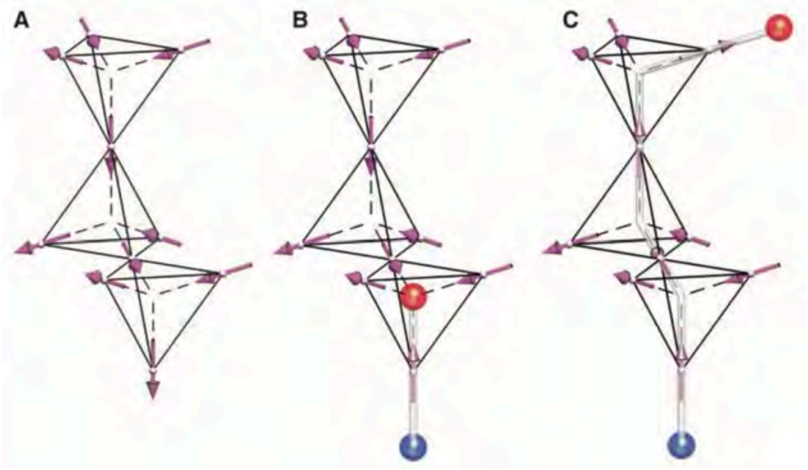

- Some magnetic systems do not order even down to very low temperatures
- often bear very interesting physics
- short-range order revealed in diffuse scattering
- most prominent example: spin ice
- highly frustrated although ferromagnetic
- *pinch points* in diffuse scattering pattern perfectly reproduced by Monte Carlo analysis
- excitations interpreted as magnetic monopoles

Short-range order

Diffuse scattering, RMC and mPDF

- $SrGd_2O_4$ containing natural Gd
- T_N = 2.73 K
- λ = 0.5 Å, Q_{max} = 7 Å^{-1}
- 50 K background subtracted

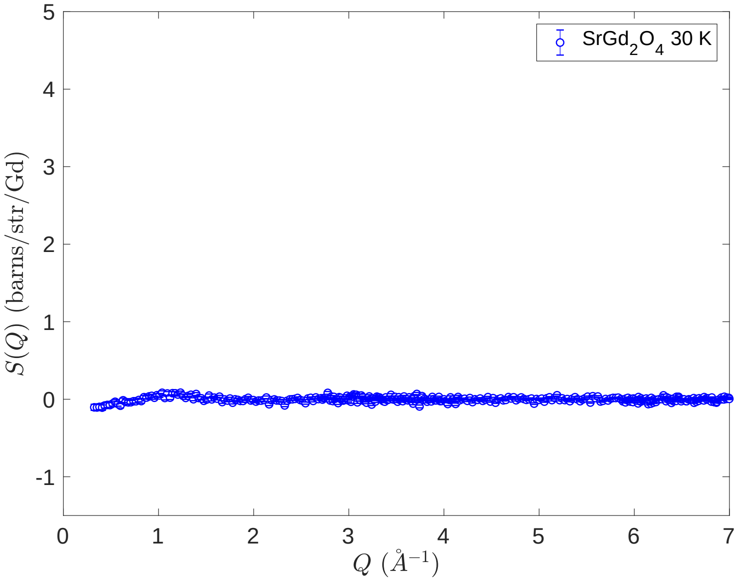

Short-range order

Diffuse scattering, RMC and mPDF

- $SrGd_2O_4$ containing natural Gd
- T_N = 2.73 K
- λ = 0.5 Å, Q_{max} = 7 $Å^{-1}$
- 50 K background subtracted

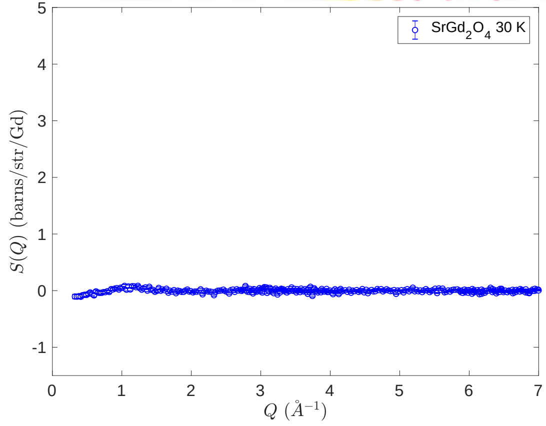

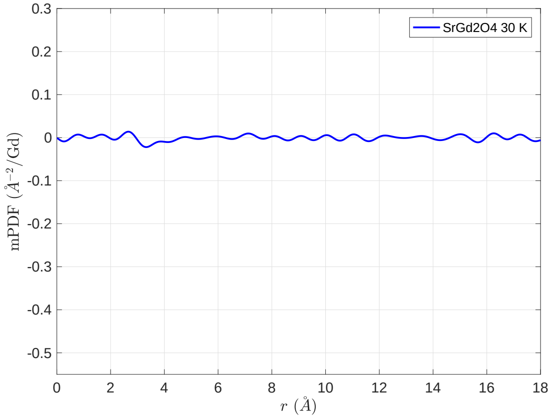

Short-range order

Diffuse scattering, RMC and mPDF

- $SrGd_2O_4$ containing natural Gd
- T_N = 2.73 K
- λ = 0.5 Å, Q_{max} = 7 $Å^{-1}$
- 50 K background subtracted

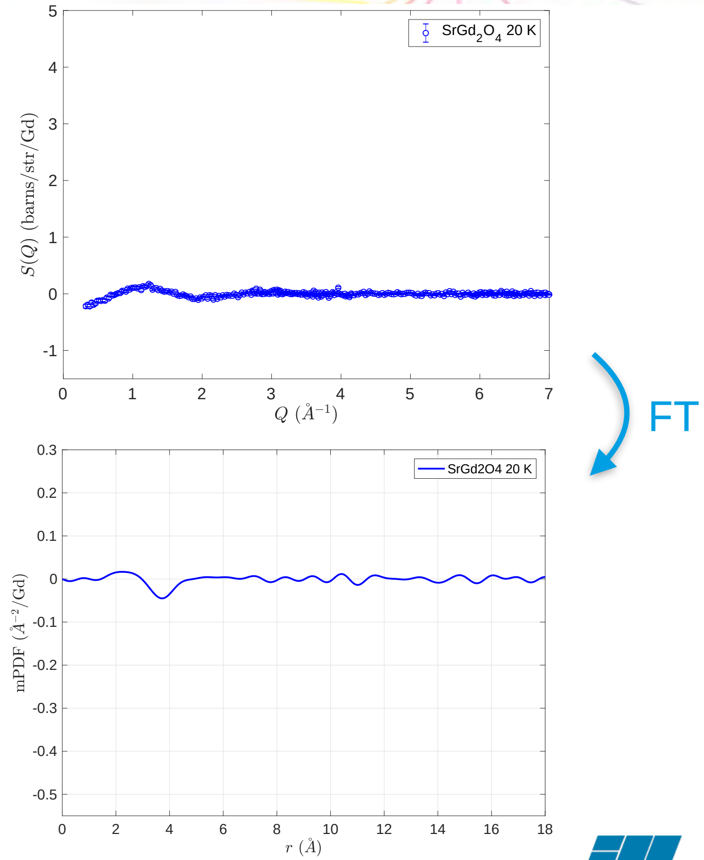

Short-range order

Diffuse scattering, RMC and mPDF

- $SrGd_2O_4$ containing natural Gd
- T_N = 2.73 K
- λ = 0.5 Å, Q_{max} = 7 Å^{-1}
- 50 K background subtracted

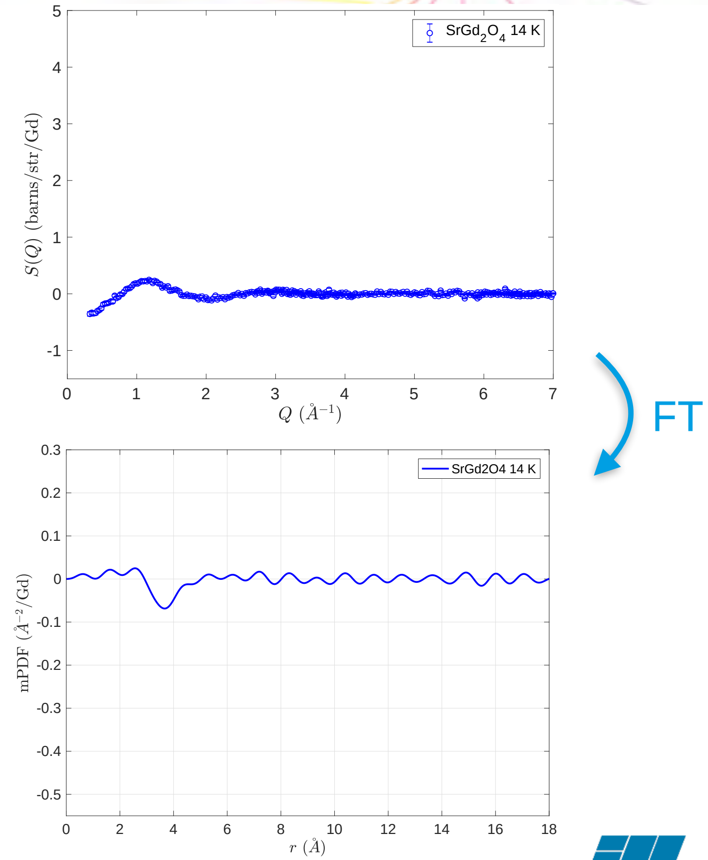

Short-range order

Diffuse scattering, RMC and mPDF

- $SrGd_2O_4$ containing natural Gd
- T_N = 2.73 K
- λ = 0.5 Å, Q_{max} = 7 Å^{-1}
- 50 K background subtracted

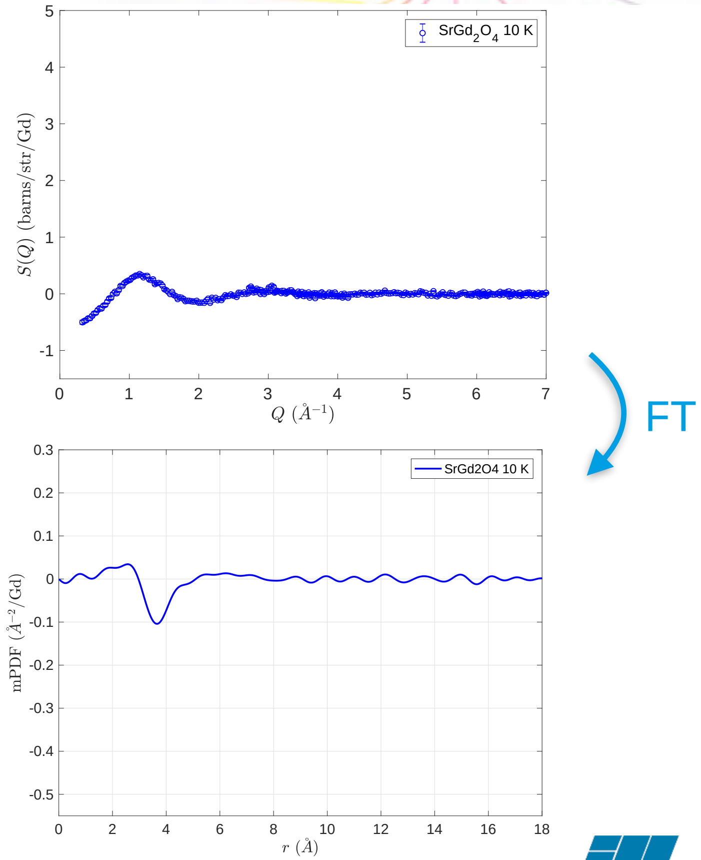

Short-range order

Diffuse scattering, RMC and mPDF

- $SrGd_2O_4$ containing natural Gd
- T_N = 2.73 K
- λ = 0.5 Å, Q_{max} = 7 Å^{-1}
- 50 K background subtracted

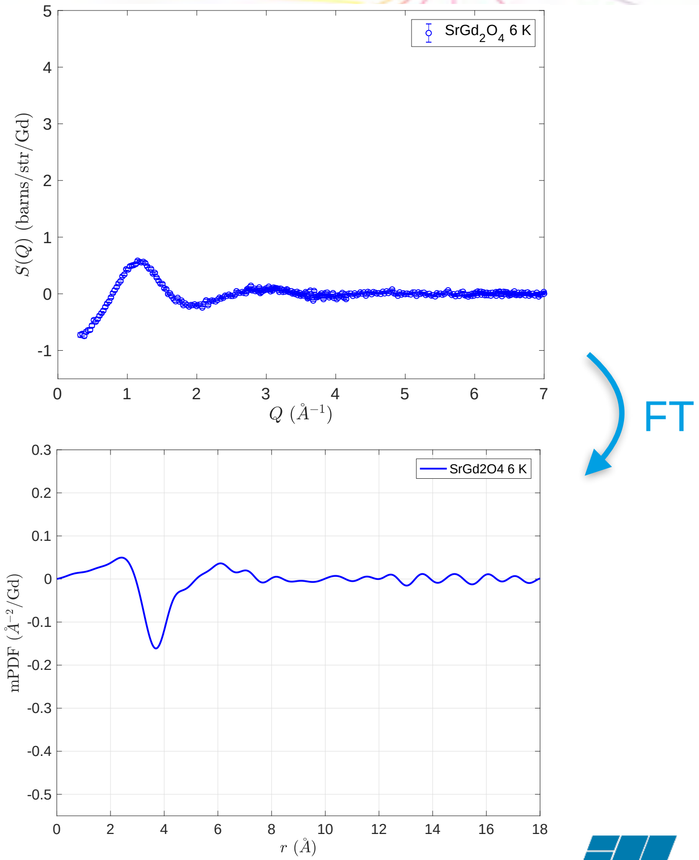

Short-range order

Diffuse scattering, RMC and mPDF

- $SrGd_2O_4$ containing natural Gd
- T_N = 2.73 K
- λ = 0.5 Å, Q_{max} = 7 $Å^{-1}$
- 50 K background subtracted

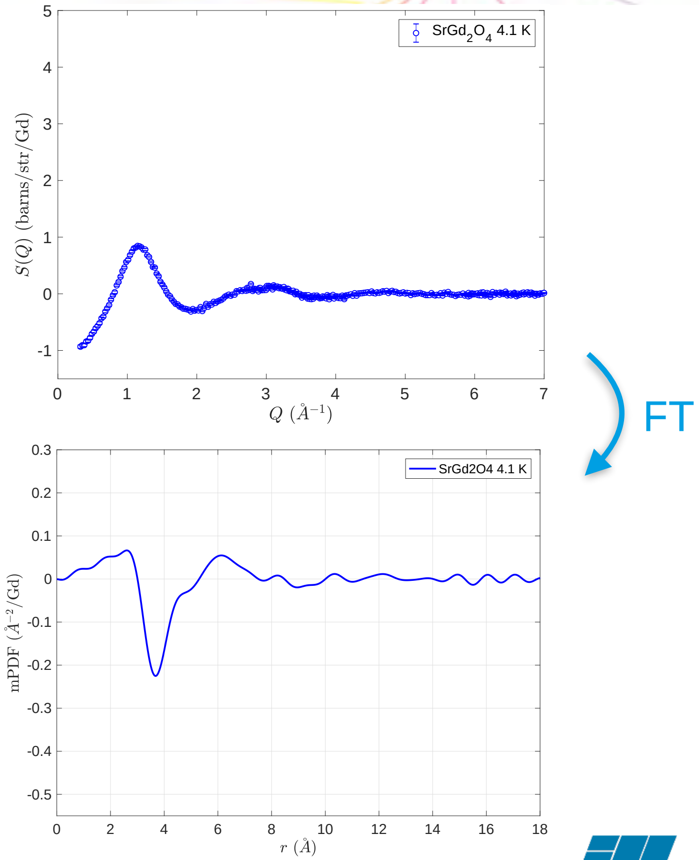

Short-range order

Diffuse scattering, RMC and mPDF

- $SrGd_2O_4$ containing natural Gd
- T_N = 2.73 K
- λ = 0.5 Å, Q_{max} = 7 $Å^{-1}$
- 50 K background subtracted

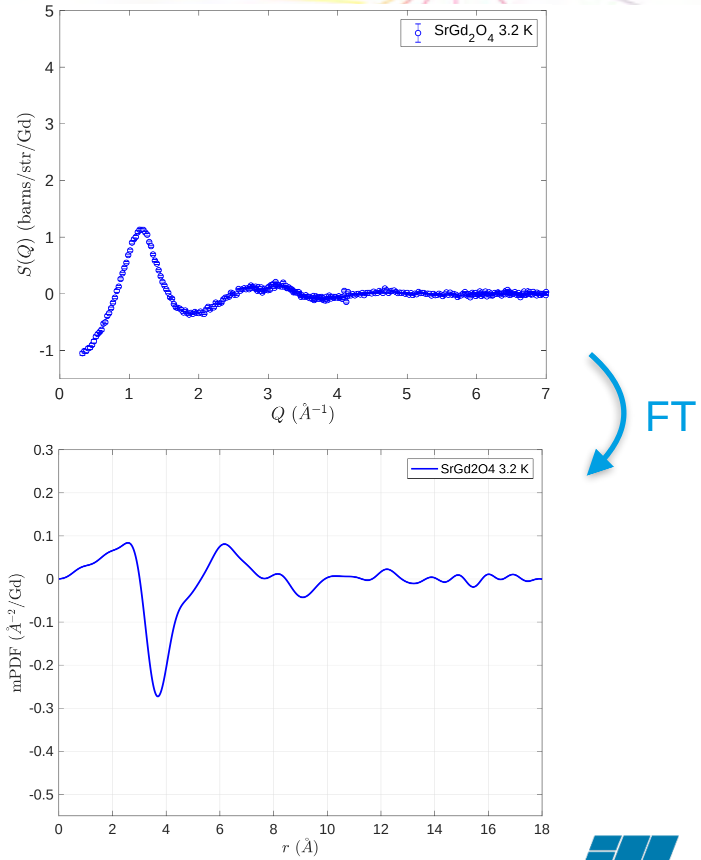

Short-range order

Diffuse scattering, RMC and mPDF

- $SrGd_2O_4$ containing natural Gd
- T_N = 2.73 K
- λ = 0.5 Å, Q_{max} = 7 Å^{-1}
- 50 K background subtracted

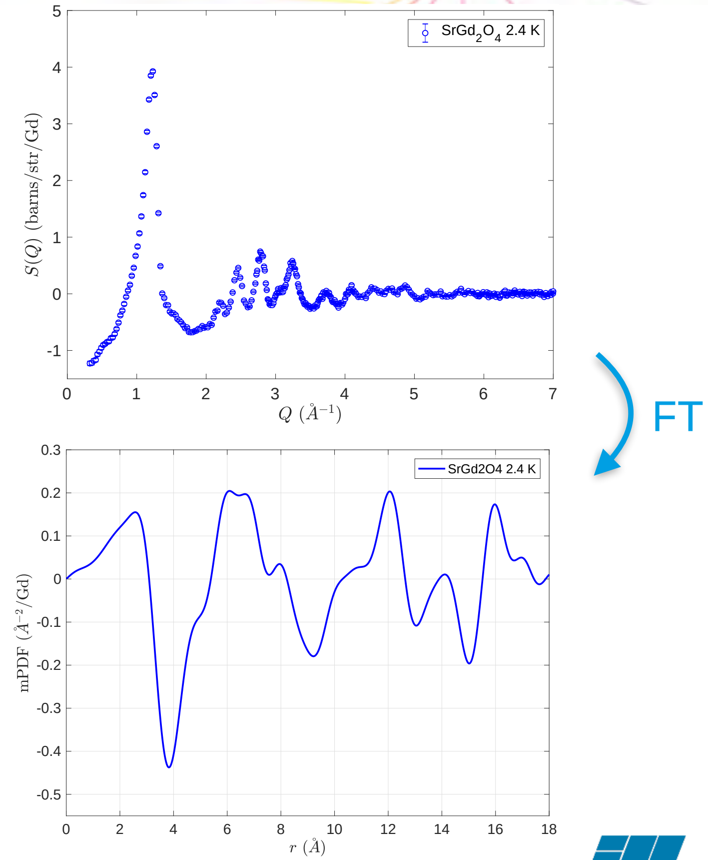

Short-range order

Diffuse scattering, RMC and mPDF

- $SrGd_2O_4$ containing natural Gd
- T_N = 2.73 K
- λ = 0.5 Å, Q_{max} = 7 $Å^{-1}$
- 50 K background subtracted

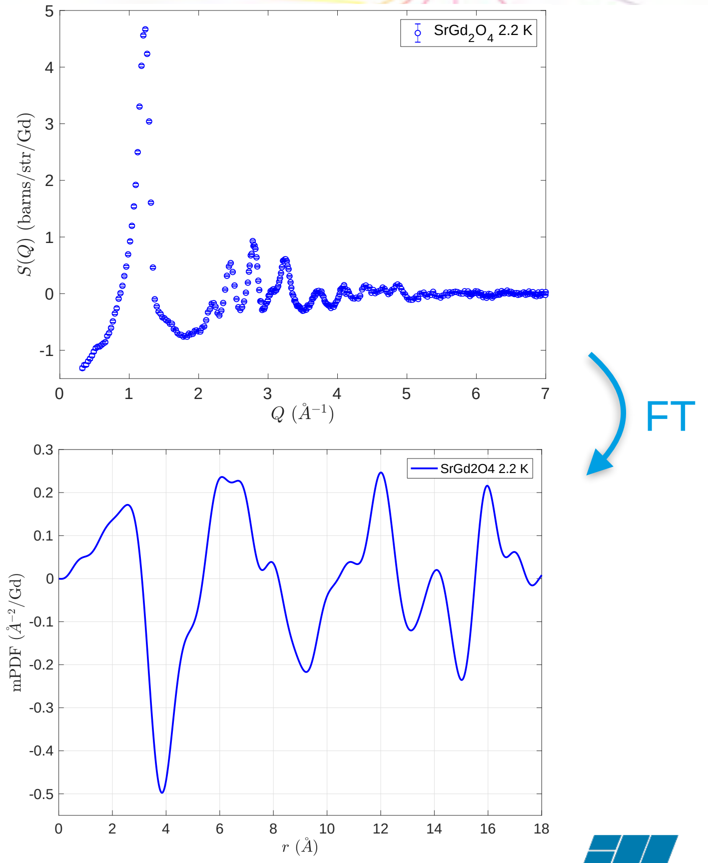

Short-range order

Diffuse scattering, RMC and mPDF

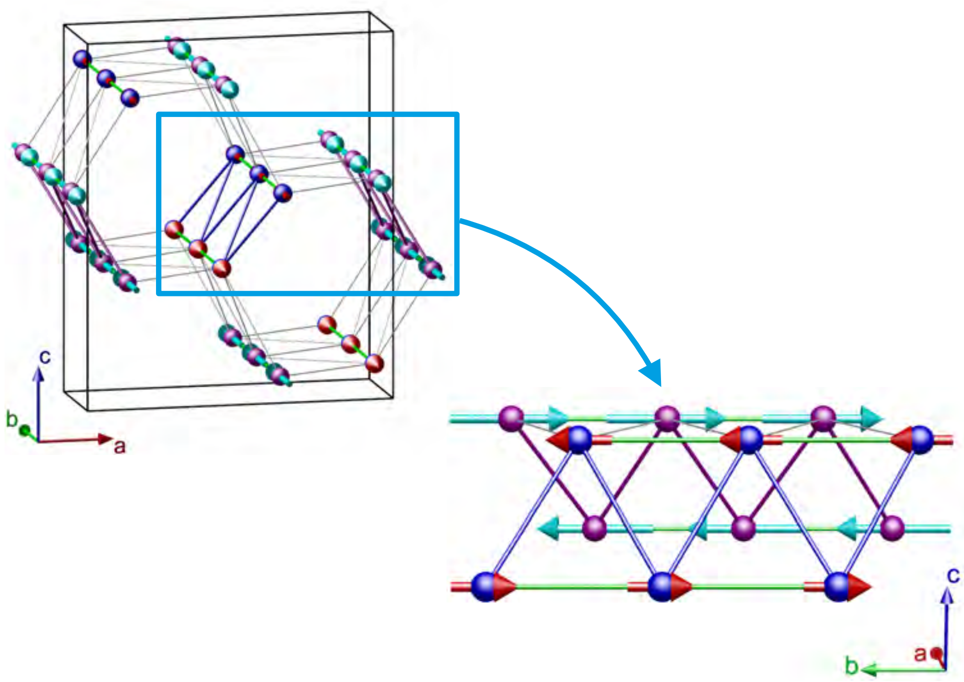

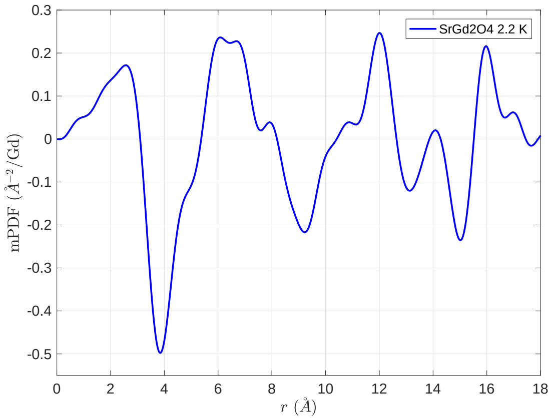

Short-range order

Diffuse scattering, RMC and mPDF

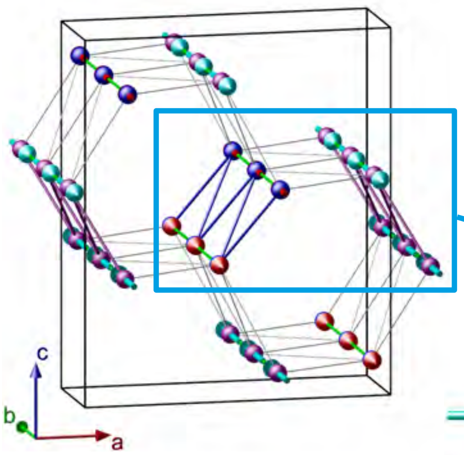

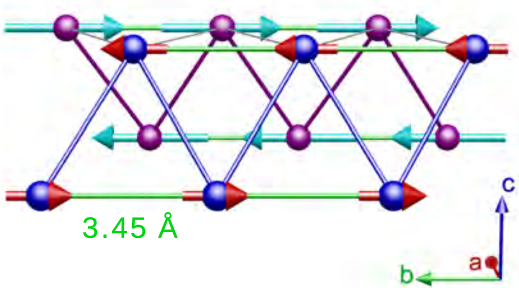

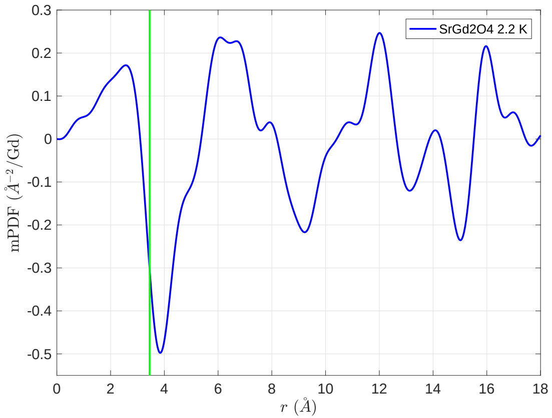

Short-range order

Diffuse scattering, RMC and mPDF

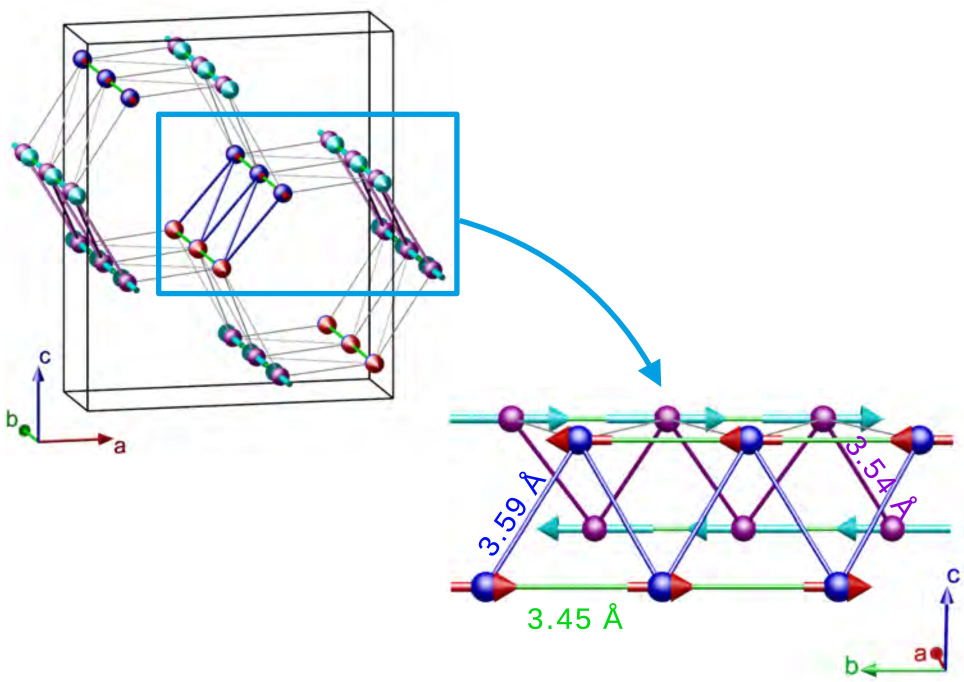

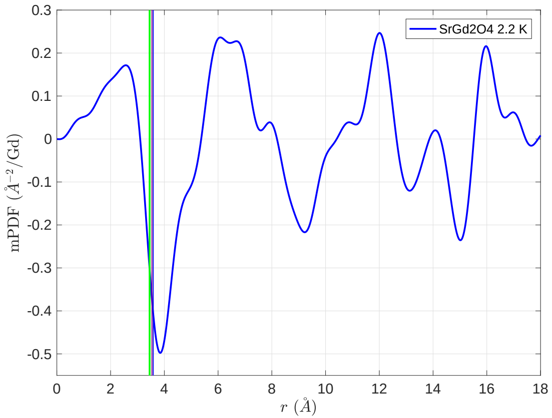

Short-range order

Diffuse scattering, RMC and mPDF

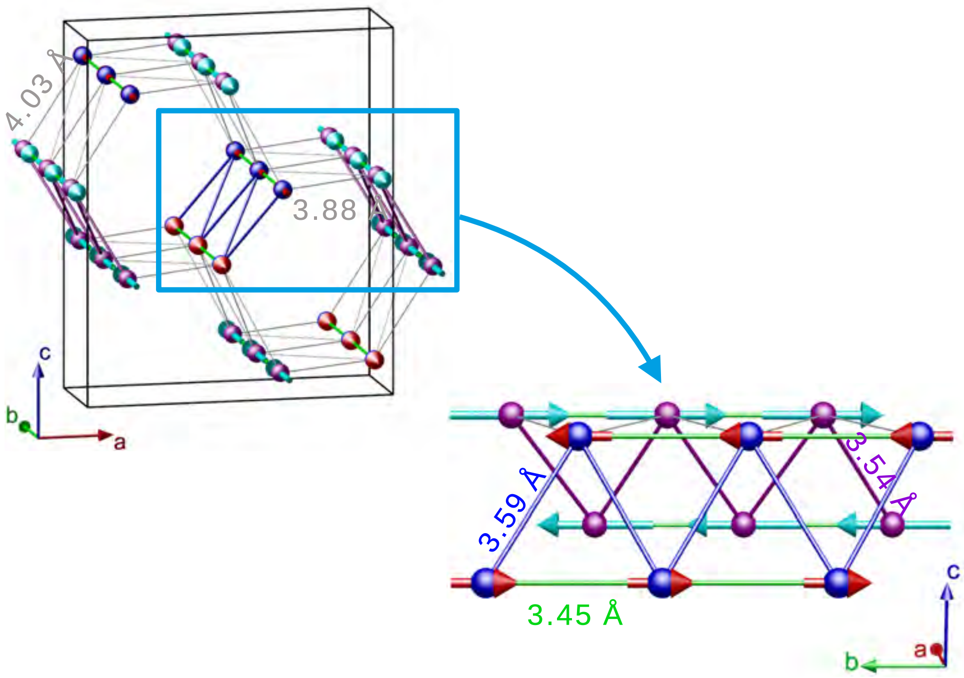

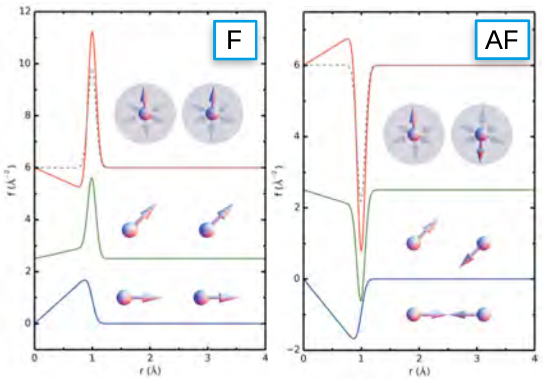

Frandsen et al., Acta Cryst. A**70** 3 (2013)

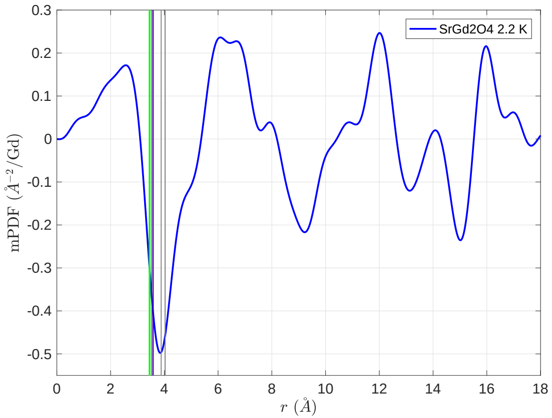

Short-range order

Diffuse scattering, RMC and mPDF

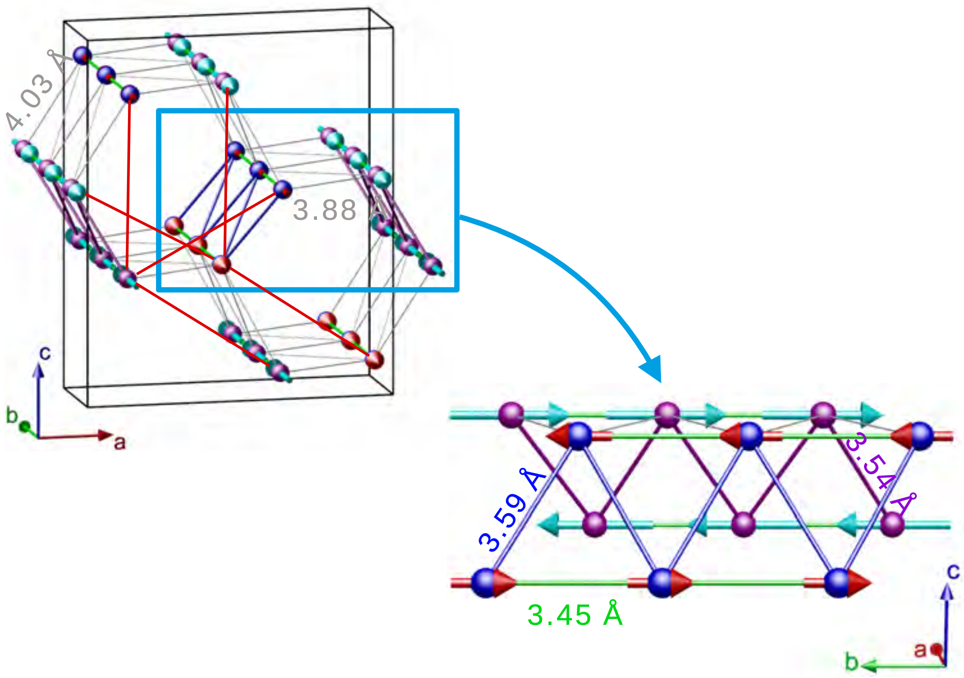

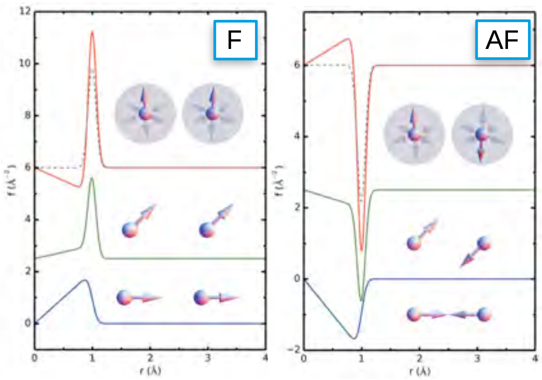

Frandsen et al., Acta Cryst. A**70** 3 (2013)

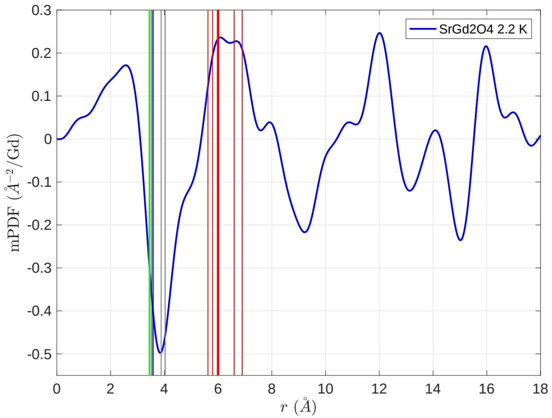

Short-range order

Diffuse scattering, RMC and mPDF

- Ising anisotropy
- $g_j \sqrt{J(J+1)}\mu_B = 7.94\mu_B$
- 9x27x9 super cell, adapted to coherence volume on D4

$$I(Q) = C[\mu f(Q)]^2 \cdot \frac{1}{N} \sum_{i,j} \left[A_{ij} \frac{\sin Qr_{ij}}{Qr_{ij}} + B_{ij} \left(\frac{\sin Qr_{ij}}{(Qr_{ij})^2} - \frac{\cos Qr_{ij}}{(Qr_{ij})^2} \right) \right]$$

$$A_{ij} = S_i^x S_j^x \qquad B_{ij} = 2S_i^z S_j^z - S_i^x S_j^x$$

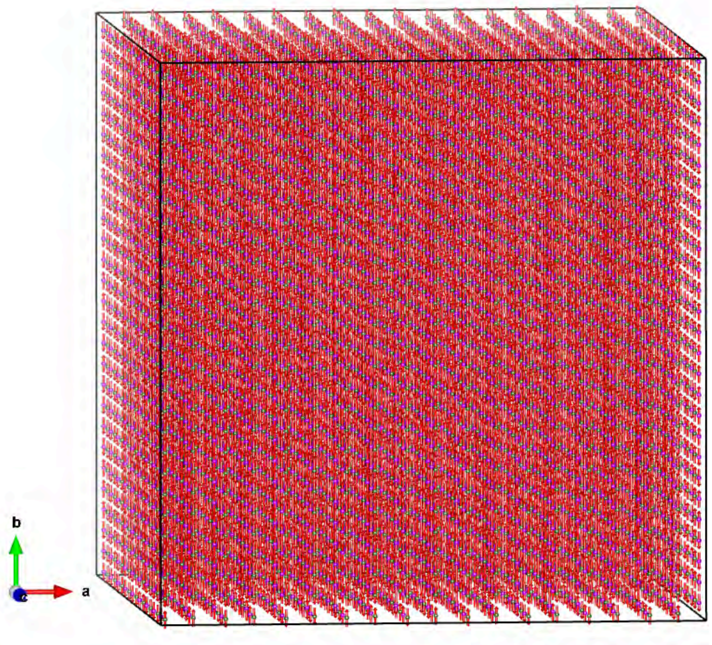

Spinvert

17496 spins

Paddison et al., J. Phys.: Condens. Matter 25, 454220 (2013)

Short-range order

Diffuse scattering, RMC and mPDF

- Ising anisotropy
- $g_j\sqrt{J(J+1)}\mu_B = 7.94\mu_B$
- 9x27x9 super cell, adapted to coherence volume on D4

$$I(Q) = C[\mu f(Q)]^2 \cdot \frac{1}{N}\sum_{i,j}\left[A_{ij}\frac{\sin Qr_{ij}}{Qr_{ij}} + B_{ij}\left(\frac{\sin Qr_{ij}}{(Qr_{ij})^2} - \frac{\cos Qr_{ij}}{(Qr_{ij})^2}\right)\right]$$

$$A_{ij} = S_i^x S_j^x \qquad B_{ij} = 2S_i^z S_j^z - S_i^x S_j^x$$

Spinvert

Paddison et al., J. Phys.: Condens. Matter 25, 454220 (2013)

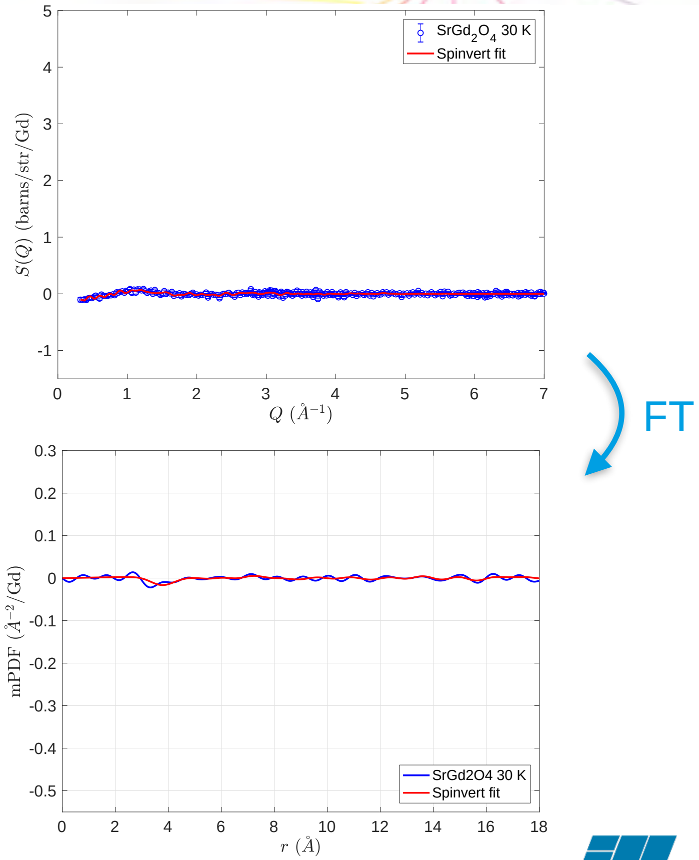

Short-range order

Diffuse scattering, RMC and mPDF

- Ising anisotropy
- $g_j \sqrt{J(J+1)}\mu_B = 7.94\mu_B$
- 9x27x9 super cell, adapted to coherence volume on D4

$$I(Q) = C[\mu f(Q)]^2 \cdot \frac{1}{N} \sum_{i,j} \left[A_{ij} \frac{\sin Qr_{ij}}{Qr_{ij}} + B_{ij} \left(\frac{\sin Qr_{ij}}{(Qr_{ij})^2} - \frac{\cos Qr_{ij}}{(Qr_{ij})^2} \right) \right]$$

$$A_{ij} = S_i^x S_j^x \qquad B_{ij} = 2S_i^z S_j^z - S_i^x S_j^x$$

Spinvert

Paddison et al., J. Phys.: Condens. Matter 25, 454220 (2013)

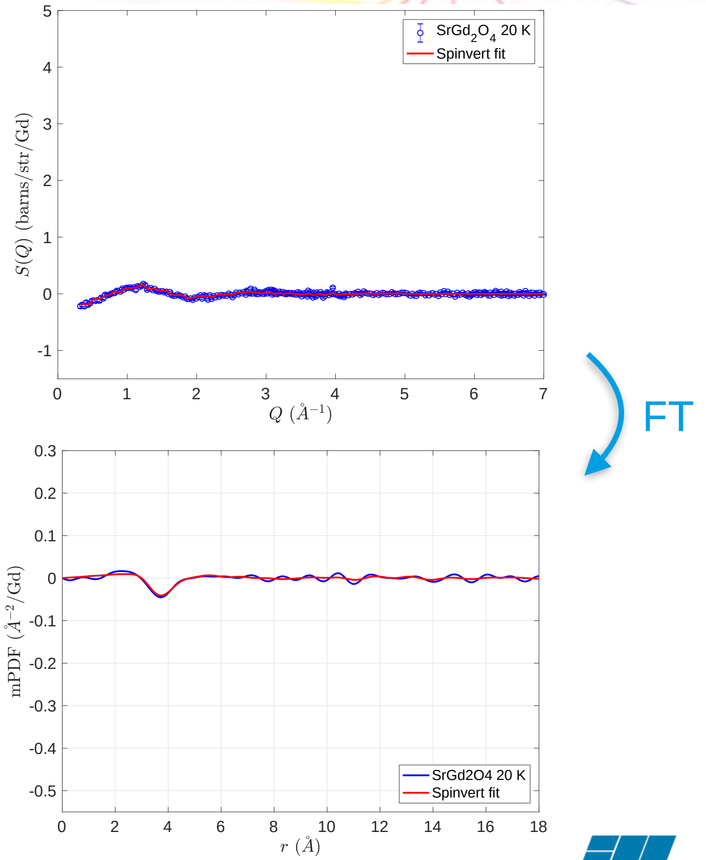

Short-range order

Diffuse scattering, RMC and mPDF

- Ising anisotropy
- $g_j\sqrt{J(J+1)}\mu_B = 7.94\mu_B$
- 9x27x9 super cell, adapted to coherence volume on D4

$$I(Q) = C[\mu f(Q)]^2 \cdot \frac{1}{N}\sum_{i,j}\left[A_{ij}\frac{\sin Qr_{ij}}{Qr_{ij}} + B_{ij}\left(\frac{\sin Qr_{ij}}{(Qr_{ij})^2} - \frac{\cos Qr_{ij}}{(Qr_{ij})^2}\right)\right]$$

$$A_{ij} = S_i^x S_j^x \qquad B_{ij} = 2S_i^z S_j^z - S_i^x S_j^x$$

Spinvert

Paddison et al., J. Phys.: Condens. Matter 25, 454220 (2013)

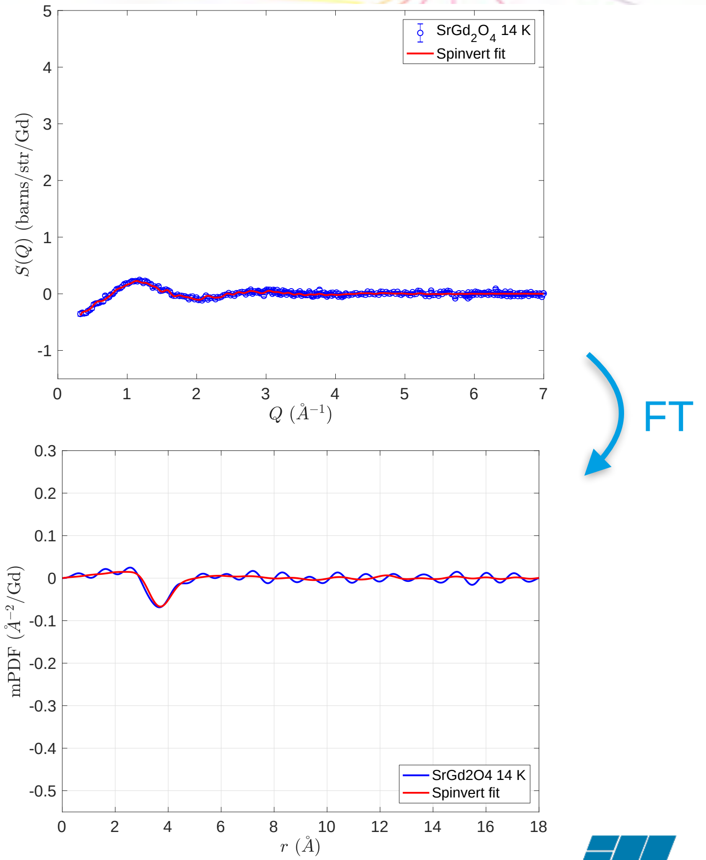

Short-range order

Diffuse scattering, RMC and mPDF

- Ising anisotropy
- $g_j\sqrt{J(J+1)}\mu_B = 7.94\mu_B$
- 9x27x9 super cell, adapted to coherence volume on D4

$$I(Q) = C[\mu f(Q)]^2 \cdot \frac{1}{N}\sum_{i,j}\left[A_{ij}\frac{\sin Qr_{ij}}{Qr_{ij}} + B_{ij}\left(\frac{\sin Qr_{ij}}{(Qr_{ij})^2} - \frac{\cos Qr_{ij}}{(Qr_{ij})^2}\right)\right]$$

$$A_{ij} = S_i^x S_j^x \qquad B_{ij} = 2S_i^z S_j^z - S_i^x S_j^x$$

Spinvert

Paddison et al., J. Phys.: Condens. Matter 25, 454220 (2013)

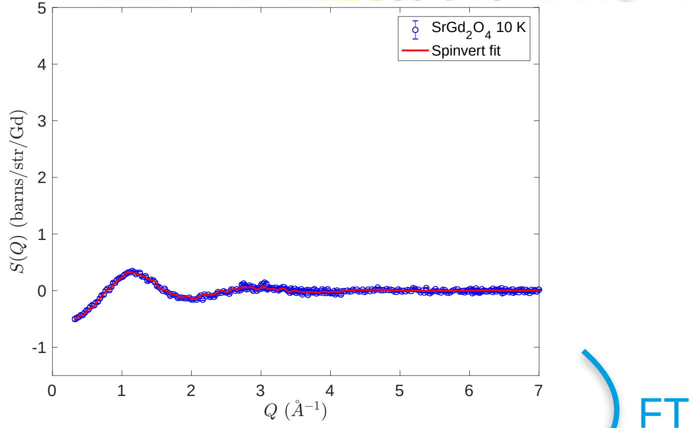

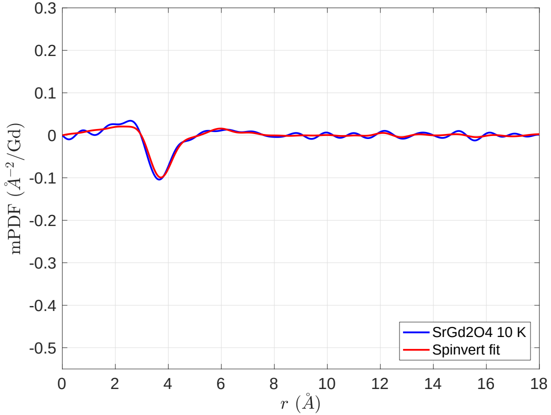

Short-range order

Diffuse scattering, RMC and mPDF

- Ising anisotropy
- $g_j\sqrt{J(J+1)}\mu_B = 7.94\mu_B$
- 9x27x9 super cell, adapted to coherence volume on D4

$$I(Q) = C[\mu f(Q)]^2 \cdot \frac{1}{N}\sum_{i,j}\left[A_{ij}\frac{\sin Qr_{ij}}{Qr_{ij}} + B_{ij}\left(\frac{\sin Qr_{ij}}{(Qr_{ij})^2} - \frac{\cos Qr_{ij}}{(Qr_{ij})^2}\right)\right]$$

$$A_{ij} = S_i^x S_j^x \qquad B_{ij} = 2S_i^z S_j^z - S_i^x S_j^x$$

Spinvert

Paddison et al., J. Phys.: Condens. Matter 25, 454220 (2013)

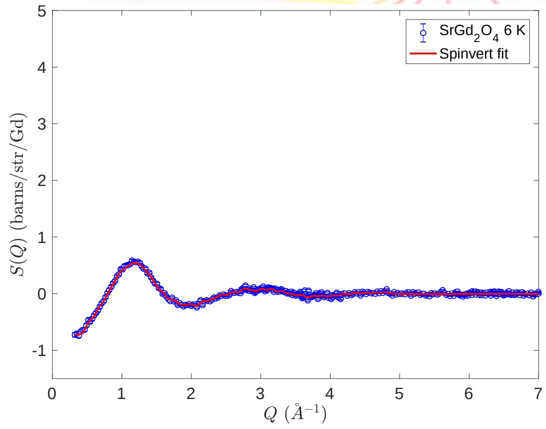

FT

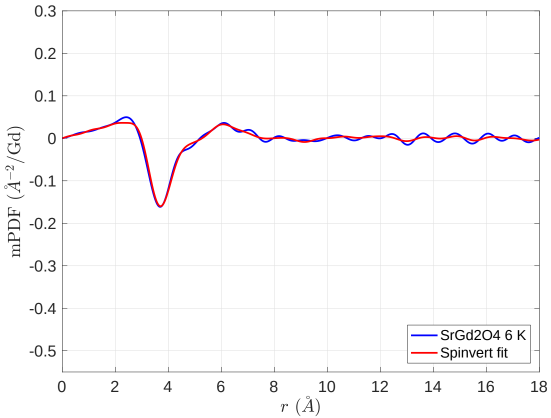

Short-range order

Diffuse scattering, RMC and mPDF

- Ising anisotropy
- $g_j\sqrt{J(J+1)}\mu_B = 7.94\mu_B$
- 9x27x9 super cell, adapted to coherence volume on D4

$$I(Q) = C[\mu f(Q)]^2 \cdot \frac{1}{N}\sum_{i,j}\left[A_{ij}\frac{\sin Qr_{ij}}{Qr_{ij}} + B_{ij}\left(\frac{\sin Qr_{ij}}{(Qr_{ij})^2} - \frac{\cos Qr_{ij}}{(Qr_{ij})^2}\right)\right]$$

$$A_{ij} = S_i^x S_j^x \qquad B_{ij} = 2S_i^z S_j^z - S_i^x S_j^x$$

Spinvert

Paddison et al., J. Phys.: Condens. Matter 25, 454220 (2013)

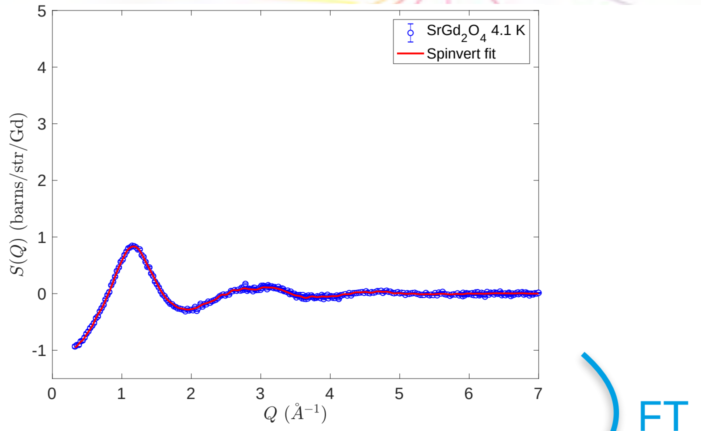

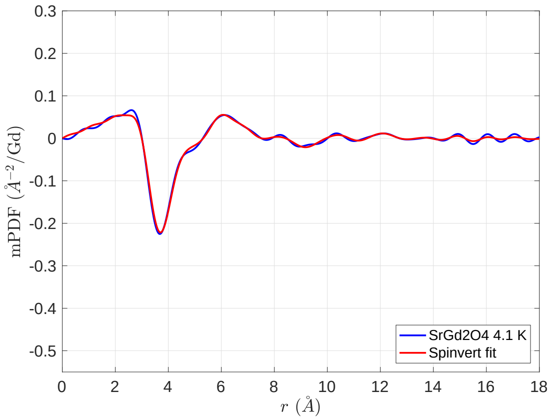

Short-range order

Diffuse scattering, RMC and mPDF

- Ising anisotropy
- $g_j\sqrt{J(J+1)}\mu_B = 7.94\mu_B$
- 9x27x9 super cell, adapted to coherence volume on D4

$$I(Q) = C[\mu f(Q)]^2 \cdot \frac{1}{N}\sum_{i,j}\left[A_{ij}\frac{\sin Qr_{ij}}{Qr_{ij}} + B_{ij}\left(\frac{\sin Qr_{ij}}{(Qr_{ij})^2} - \frac{\cos Qr_{ij}}{(Qr_{ij})^2}\right)\right]$$

$$A_{ij} = S_i^x S_j^x \qquad B_{ij} = 2S_i^z S_j^z - S_i^x S_j^x$$

Spinvert

Paddison et al., J. Phys.: Condens. Matter 25, 454220 (2013)

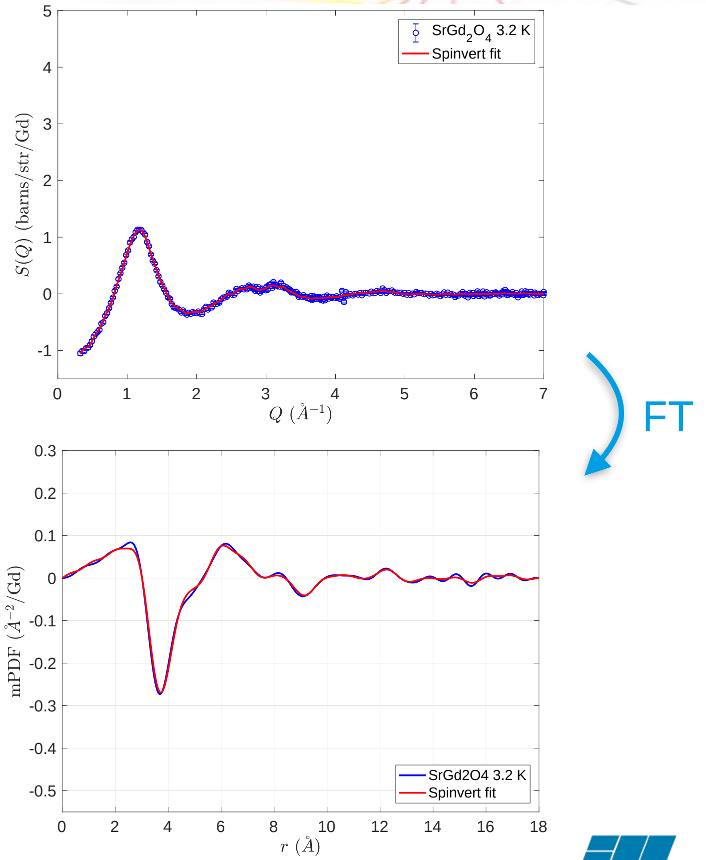

Short-range order

Diffuse scattering, RMC and mPDF

- Ising anisotropy
- $g_j\sqrt{J(J+1)}\mu_B = 7.94\mu_B$
- 9x27x9 super cell, adapted to coherence volume on D4

$$I(Q) = C[\mu f(Q)]^2 \cdot \frac{1}{N}\sum_{i,j}\left[A_{ij}\frac{\sin Qr_{ij}}{Qr_{ij}} + B_{ij}\left(\frac{\sin Qr_{ij}}{(Qr_{ij})^2} - \frac{\cos Qr_{ij}}{(Qr_{ij})^2}\right)\right]$$

$$A_{ij} = S_i^x S_j^x \qquad B_{ij} = 2S_i^z S_j^z - S_i^x S_j^x$$

Spinvert

Paddison et al., J. Phys.: Condens. Matter 25, 454220 (2013)

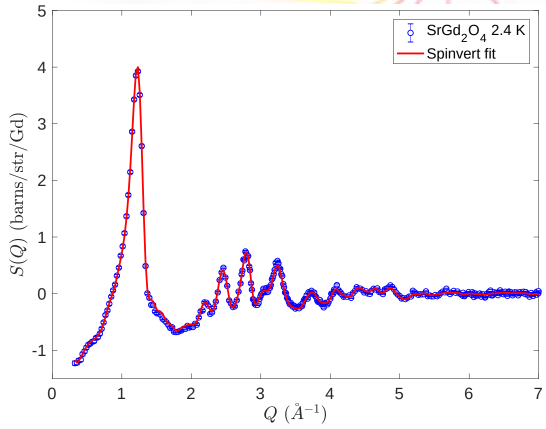

FT

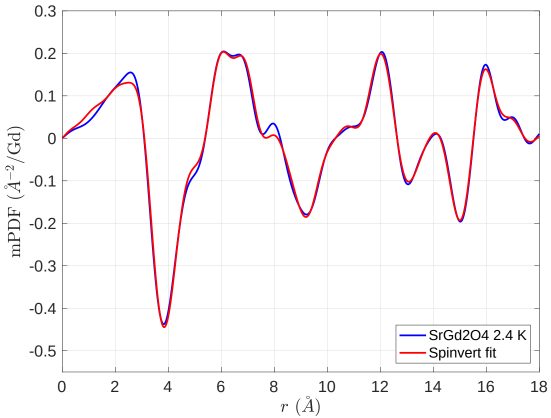

Short-range order

Diffuse scattering, RMC and mPDF

- Ising anisotropy
- $g_j\sqrt{J(J+1)}\mu_B = 7.94\mu_B$
- 9x27x9 super cell, adapted to coherence volume on D4

$$I(Q) = C[\mu f(Q)]^2 \cdot \frac{1}{N}\sum_{i,j}\left[A_{ij}\frac{\sin Qr_{ij}}{Qr_{ij}} + B_{ij}\left(\frac{\sin Qr_{ij}}{(Qr_{ij})^2} - \frac{\cos Qr_{ij}}{(Qr_{ij})^2}\right)\right]$$

$$A_{ij} = S_i^x S_j^x \qquad B_{ij} = 2S_i^z S_j^z - S_i^x S_j^x$$

Spinvert

Paddison et al., J. Phys.: Condens. Matter 25, 454220 (2013)

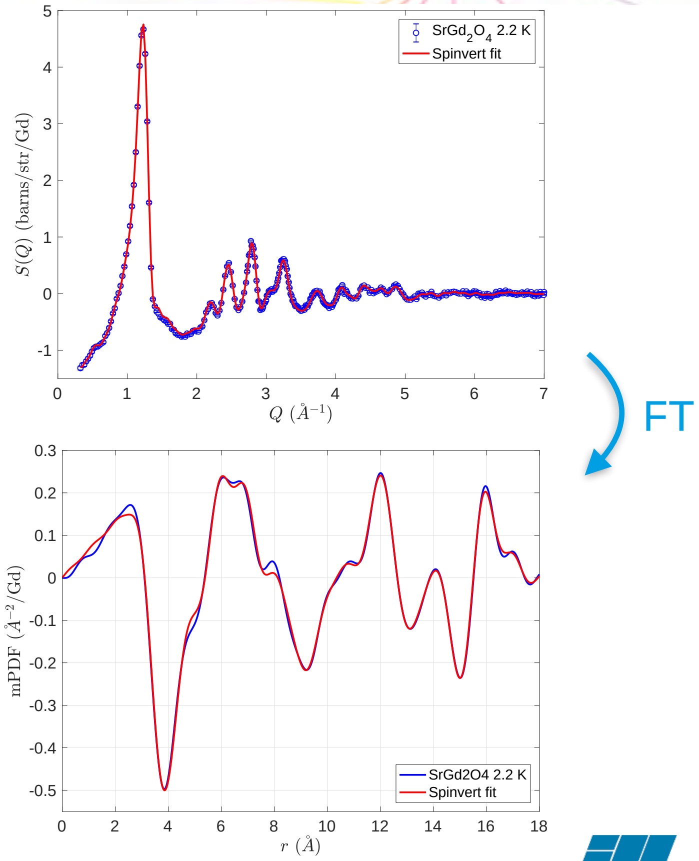

Short-range order

Diffuse scattering, RMC and mPDF

- Ising anisotropy
- $g_j\sqrt{J(J+1)}\mu_B = 7.94\mu_B$
- 9x27x9 super cell, adapted to coherence volume on D4

$$I(Q) = C[\mu f(Q)]^2 \cdot \frac{1}{N}\sum_{i,j}\left[A_{ij}\frac{\sin Qr_{ij}}{Qr_{ij}} + B_{ij}\left(\frac{\sin Qr_{ij}}{(Qr_{ij})^2} - \frac{\cos Qr_{ij}}{(Qr_{ij})^2}\right)\right]$$

$$A_{ij} = S_i^x S_j^x \qquad B_{ij} = 2S_i^z S_j^z - S_i^x S_j^x$$

Spinvert

Paddison et al., J. Phys.: Condens. Matter 25, 454220 (2013)

spin-spin correlation function

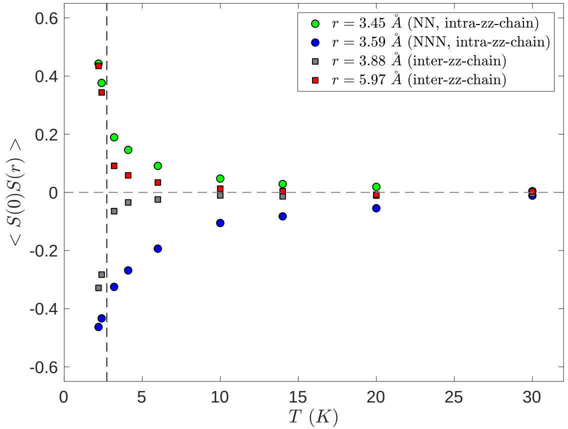

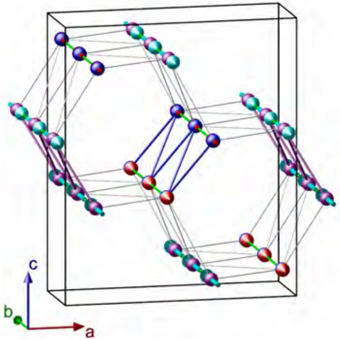

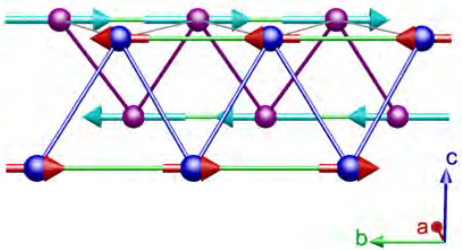

Large-scale structures

Small angle neutron scattering (SANS)

- Large-scale structures up to 5000 Å —> low q —> SANS
- Skyrmions (particle-like objects described as magnetic hedgehogs)
- Flux line lattices in superconductors

Mühlbauer et al., Science **323** 915 (2011)

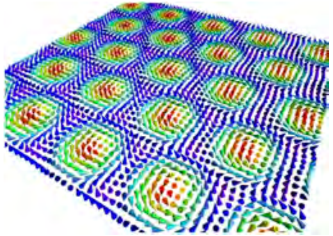

taken from riken.jp

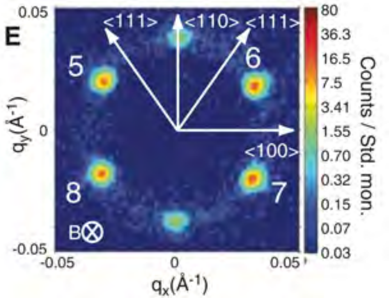

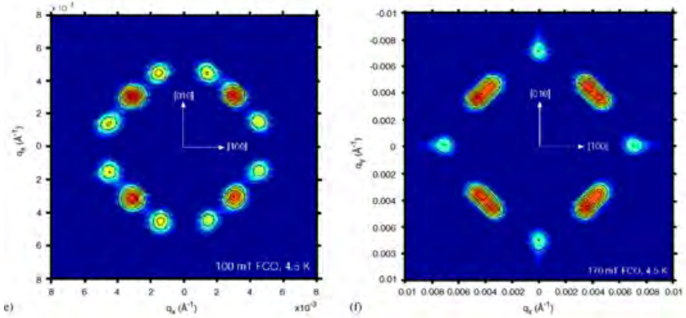

Dewhurst et al., *Physica B* **385** 176 (2006)

Phonons and magnons

Inelastic neutron scattering

- Lattice dynamics, atomic forces
- Spin waves, magnetic exchange parameters

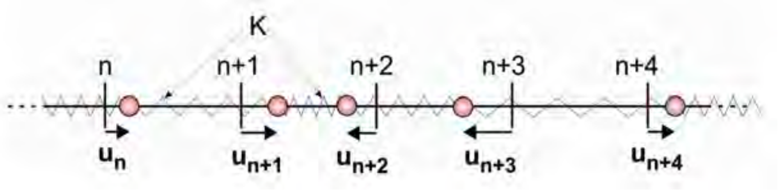

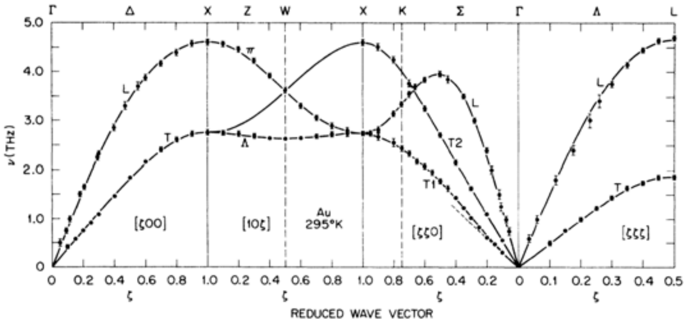

Lynn et al., *Phys. Rev. B* **8** 3493 (1973)

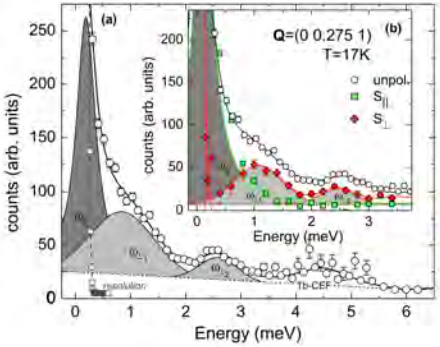

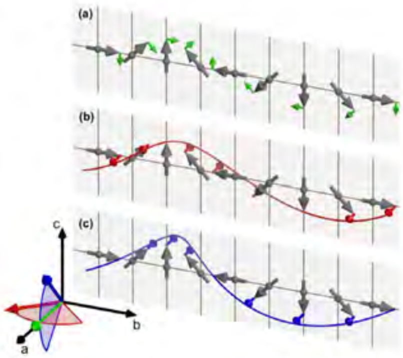

Senff et al., *J. Phys.: Condens. Matt.* **20** 434212 (2008)

NEUTRONS
FOR SOCIETY

I N S T I T U T   L A U E   L A N G E V I N

T H E   E U R O P E A N   N E U T R O N   S O U R C E

NEUTRONS
FOR SOCIETY